For Journal of Phycology

Article type: Research Article

Title

PHYLOGEOGRAPHY OF A CANOPY-FORMING KELP, *EISENIA BICYCLIS* (LAMINARIALES, PHAEOPHYCEAE), BASED ON A GENOME-WIDE SEQUENCING ANALYSIS [1]

List of Authors and Affiliations

Kanako Chimura

Humanities and Science, Ochanomizu University, 2-1-1 Otsuka Bunkyoku, Tokyo 112-8610, Japan.

Shingo Akita (ORCID: 0000-0003-1140-2593) [2]

Natural Science, Ochanomizu University, 2-1-1 Otsuka Bunkyoku, Tokyo 112-8610, Japan.

Faculty of Fisheries Sciences, Hokkaido University, 3-1-1 Minato, Hakodate, Hokkaido 041-8611, Japan

Takaya Iwasaki (ORCID: 0000-0002-2194-4153)

Natural Science, Ochanomizu University, 2-1-1 Otsuka Bunkyoku, Tokyo 112-8610, Japan.

Atsushi J. Nagano (ORCID: 0000-0001-7891-5049)

Faculty of Agriculture, Ryukoku University, Yokotani 1-5, Seta Ohe-cho, Otsu, Shiga, 520-2194, Japan.

Institute for Advanced Biosciences, Keio University, 403-1 Nipponkoku, Daihouji, Tsuruoka, Yamagata, 997-0017, Japan

Satoshi Shimada [3] (ORCID: 0000-0003-4810-4303)

Natural Science, Ochanomizu University, 2-1-1 Otsuka Bunkyoku, Tokyo 112-8610, Japan.

[2] Corresponding author

E-mail address: sakitam@fish.hokudai.ac.jp

TEL. & FAX: 81-138-40-5532

[3] Shared corresponding author

E-mail address: shimada.satoshi@ocha.ac.jp

TEL. & FAX: 81-3-5978-5356

Running title:

PHYLOGEOGRAPHY OF *E. BICYCLIS*

ABSTRACT

Analyses of phylogeographic patterns and genetic diversity provide fundamental information for the management and conservation of species. However, little is published about these patterns in Japanese kelp species. In this study, we conducted phylogeographic analyses of a canopy-forming kelp, *Eisenia bicyclis*, based on genome-wide SNPs identified by ddRAD-seq. We obtained 1,299 SNPs for 76 samples from nine localities across the distribution. STRUCTURE, NeighborNet, and discriminant analysis of principal components consistently showed high genetic differentiation among the Eastern Pacific, Central Pacific, and Sea of Japan coastal regions. Relatively strong gene flow was detected only within populations in the Eastern Pacific and in the Sea of Japan. Genetic diversity and genetic uniqueness were high in the Central Pacific and low in the Sea of Japan. These results suggest that there were at least three independent refugia corresponding to the three regions during the Last Glacial Maximum (LGM). Furthermore, relatively larger populations in the Central Pacific and smaller populations in the Sea of Japan have been maintained in the demographic history from before the LGM to the present. These phylogeographic histories were supported by an Approximate Bayesian Computation analysis. From a conservation genetics perspective, the loss of southern populations in the Central Pacific would greatly reduce the total genetic diversity of the species. Southern populations in the Sea of Japan, which have relatively low genetic diversity, may be highly vulnerable to environmental change, such as heat waves and increased feeding. Therefore, careful monitoring and conservation are needed in the two regions.

Key index words:

Arthrothamnaceae, ddRAD-seq, Demography, Genetic diversity, Genetic structure, Kelp forest, Phylogeography

Abbreviations:

ABC, Approximate Bayesian Computation; BIC, Bayesian information criterion; CI, confidence interval; CTAB, cetyltrimethylammonium bromide; DA, discriminant analysis; DAPC, discriminant analysis of principal components; ddRAD-seq, double digest RAD-seq; LGM, Last Glacial Maximum; PCA, principal component analysis; RAD-seq, restriction site-associated DNA sequencing; SNPs, single nucleotide polymorphisms; SS, summary statistics; SST, surface seawater temperature

INTRODUCTION

Kelp forests are key components of coastal rocky ecosystems in temperate to boreal zones by providing food, habitat, and shelter for various organisms (North 1971, Steneck et al. 2002, Graham 2004, Steneck and Johnson 2014). They also serve as a significant carbon sink to mitigate global warming (Chung et al. 2013, Krause-Jensen and Duarte 2016). However, kelp forests have been declining in various parts of the world (Krumhansl et al. 2016, Wernberg et al. 2019), including Japan (Fujita 2010), due to the dominance of sea urchins (Filbee-dexter and Scheibling 2014, Ling et al. 2015), overbrowsing by herbivores (Gianni et al. 2017, Zarco-Perello et al. 2017), and recent climate change (e.g., Wernberg et al. 2016, Bennet and Catton 2019, Tanaka et al. 2020). Although effective re-forestation techniques have been developed to restore kelp forests (e.g., Ling et al. 2010, Westermeier et al. 2014, Fredriksen et al. 2020), their implementation should consider intraspecific genetic diversity and genetic structure (Moritz 2002, Hoban et al. 2020). Furthermore, recent studies have reported that populations with high genetic diversity tend to show high resilience against heatwaves in kelp populations (Wernberg et al. 2018) and against disturbance by grazing geese in seagrass populations (Hughes and Stachowicz 2004). Restoration that incorporated genetic structure and diversity was demonstrated in a canopy-forming brown alga by Wood et al. (2020). The mechanism by which genetic diversity positively affects the resilience is entirely unclear, but it is likely to be one of the important factors in management of kelp forest. Thus, understanding genetic diversity and genetic structure in each kelp species will provide fundamental information for the management and conservation of kelp forests.

Phylogeographic analyses are a powerful tool to reveal genetic diversity, genetic

structures, demographic histories, and future demographic shifts (Avise 2000). Microsatellite markers and/or organellar markers are frequently employed in studies of brown algae (reviewed in Hu et al. 2016). However, these markers are limited in number, ranging from one to a dozen loci, and the resolution of the genetic structure is poor, especially in the case of species with complex demographic histories. Alternatively, genome-wide SNP information, including hundreds to thousands of loci, provides a robust and clear basis for estimating demographic histories (reviewed in Edwards et al. 2015). The recent development of RAD-seq enabled low-cost high-throughput SNP genotyping, even in non-model organisms (Miller et al. 2007). Subsequently, ddRAD-seq, which uses two restriction enzymes with rare and frequent cutting, enabled precise, repeatable size selection and more stable shared region recovery across samples compared with RAD-seq (Kai et al. 2014). In fact, the recent employment of the ddRAD-seq method for phylogeographic studies of brown algae has revealed much clearer demographic histories than those obtained with previous markers (Guzinski et al. 2018, Kobayashi et al. 2018, LeCam et al. 2020).

Eisenia bicyclis (Kjellman) Setchell is a palm-like kelp and a representative component of kelp forests in Japan (Maegawa 1990, Terada et al. 2020). This kelp occurs in the lower intertidal zone to subtidal zone at depths shallower than 10 m (Maegawa 1990, Sakanishi et al. 2018), with a geologically disconnected distribution on the Pacific coast of central to eastern Honshu and the Sea of Japan coast of north-western Honshu, northern Kyushu, and Ulleungdo island in Korea (Fig. 1) (Kawai et al. 2020). The optimal growth temperature for this kelp ranges from 10 to 20 ºC (Ohta 1988, Kurashima et al. 1996, Baba 2010). Upper survival temperature is 29 ˚C (reviewed in Baba 2021), though the tolerance varies among localities (Ohtake et al

2020) and temperatures as low as 5 ºC are tolerated, with growth rates only dropping to 80% when compared to optimal temperatures, under adequate light intensity (Kurashima et al. 1996). Further, a success in restoration (Yotsui and Maesako 1993) and afforestation (Taniguchi and Agatsuma 2001, Taniguchi et al. 2001) of *E. bicyclis* bed were reported. As described above, ecophysiological properties of this kelp have been well-documented in efforts to conserve kelp forests. However, phylogeographic and conservation genetic studies of the species have not yet been conducted and, accordingly, the genetic structure and genetic diversity are still unknown. Further, the demographic histories enable us to estimate future shifts in the distribution, as mentioned above. The purpose of the present study was to reveal the genetic structure, genetic diversity, and demographic history of the kelp using SNP markers based on ddRAD-seq.

MATERIALS & METHODS

Sampling and ddRAD-seq library construction

Eighty-eight thalli were collected from nine localities covering the southern and northern limits of the two disconnected distributions (Fig. 1, Table S1). The individuals were collected at least 1 m apart to avoid the sampling of close relatives. The samples were preserved at -30 °C until DNA extraction. Total genomic DNA was extracted using the CTAB method as described by Doyle and Doyle (1990). A ddRAD library was prepared with the *EcoR*I and *Bgl*II enzymes following a previously described protocol (Peterson et al. 2012) with slight modifications, as described in Kobayashi et al. (2018). The library was sequenced to generate 151 bp paired-end reads in one lane of HiSeq X Ten (Illumina, San Diego, CA, USA) by a DNA sequencing service (Macrogen Japan

Corp., Tokyo, Japan).

SNP calling

From the paired-end reads, only the first reads (R1) were used for subsequent analyses for the following two reasons: 1) the quality of the R2 reads was relatively poor; 2) there was no clear advantage in using adjacent SNP sites for population genetics analyses. From the raw data, trimming was carried out using Trim Galore (https://github.com/FelixKrueger/TrimGalore/). This is a wrapper script to automate quality and adapter trimming as well as quality control; it runs Cutadapt and FastQC internally. In this tool, we used Cutadapt 1.18 (Martin 2011) and FastQC v.0.11.8 (http://www.bioinformatics.babraham.ac.uk/projects/fastqc/). The trimming process included three steps. First, all raw reads from all samples were trimmed with a quality threshold of 30, minimum length of 80, and auto-detection of the adapter set. However, with this first trimming alone, many adapter sequences were detected by FastQC as overexpressed. Therefore, a second trimming step was performed with quality 30 and minimum length 100, specifying the adapter sequences detected by each FastQC check for each sample individually. Finally, the first 100 bp sequences were extracted from the 5'-end of the reads to obtain a uniform read length.

Stacks 1.48 (Catchen et al. 2011) was used to process the trimmed ddRAD-seq reads with the following parameter settings: minimum number of identical reads required to create a stack (m = 3), nucleotide mismatches between loci within a single individual (M = 2), and mismatches between loci when building the catalogue (n = 4). The SNP genotype for each individual was exported with a minimum stack depth of 5 and a maximum observed heterozygosity cutoff of 0.6. Only the first SNP in each catalogue

was retrieved to exclude highly linked SNPs from the dataset. This filtering was carried out using the 'populations' command in Stacks. The exported SNPs were filtered using TASSEL 5.2.66 (Bradbury et al. 2007) with the following conditions: loci with a minor allele frequency < 0.01, loci with a missing individual rate > 0.6, and individuals with a missing locus rate > 0.4. During these filtering procedures, 12 individuals were filtered out due to low genotyping rates. Furthermore, 177 SNPs were detected as outliers with an FDR threshold of 0.05 using R v.3.6.3 (R Core Team 2020) with the package PCAdapt (Duforet-Frebourg et al. 2014) and removed. In this outlier detection, $K = 1$ was used because the first principal component explained most of the variance. The outlier SNPs may have adaptive information. Unfortunately, in the present study, we decided not to use the outliers for further analysis. Outliers detected when using a small number of environmentally and genetically different populations would be less reliable. The remaining neutral SNPs are a good dataset that accurately shows the trend of genetic differentiation across the genome, and it was used for the subsequent analysis.

Genetic diversity

As genetic diversity parameters, the number of different alleles per locus (N_A), number of effective alleles per locus (N_E), number of private alleles (N_P), Shannon's information index (I), observed heterozygosity (H_O), expected heterozygosity (H_E), unbiased expected heterozygosity (uH_E), and inbreeding coefficient (F_{IS}) were calculated for each population using GenAlEx v.6.501 (Peakall and Smouse 2012). Allelic richness (AR) after rarefaction to the smallest sample size of N = 7 was calculated using the diveRsity package (Keenan et al. 2013) in R v.3.6.3 (R core team 2020).

The contributions of each population to allelic diversity (Caballero et al. 2010) in

198 total (A_T), within populations (A_S), and between populations (D_A) were estimated using
199 Metapop2 (López-Cortegano et al. 2019). Because allelic diversity relies on the
200 calculation of allelic richness and the dissimilarity of alleles across subpopulations
201 rather than on gene diversity (López-Cortegano et al. 2019), it is appropriate in this
202 case, in which different alleles are expected to be distributed across regions.
203
204 *Genetic structure*
205 Genetic structure was inferred using model- and distance-based methods. In the model-
206 based method, a Bayesian analysis under the admixture F model for correlated allele
207 frequencies (Falush et al. 2003) was conducted using STRUCTURE v.2.3.4 (Pritchard
208 et al. 2000). Clusters (K) from K = 1 to 10 were estimated with a burn-in of 100,000
209 followed by 100,000 Markov chain Monte Carlo repetitions, without a priori population
210 assignment of individuals. Twenty independent runs were performed for each K value.
211 Then, the meaningful number of genetic clusters (K) was determined based on a
212 combination of the mean Ln probability of the data (LnP(K)) (Pritchard et al. 2000) and
213 the second-order rate of change in the log probability of the data (ΔK) (Evanno et al.
214 2005). The ΔK values were calculated using STRUCTURE HARVESTER v.0.6.94
215 (Earl and von Holdt 2012). For each cluster, H_E and F_{ST} values were calculated using
216 STRUCTURE to estimate genetic diversity and genetic drift from a common ancestral
217 population, respectively. The F_{ST} values in STRUCTURE are analogous to traditional
218 F_{ST} values between a cluster and a common ancestral population; see the user manual
219 for STRUCTURE (Pritchard et al. 2010).
220 In the distance-based analysis, we used DAPC, a multivariate method based on
221 sequential K means clustering and model selection that does not assume any genetic

model (Jombart et al. 2010), implemented in the adegenet 2.0.1 package (Jombart and Ahmed 2011) in R v.3.2.3. (R core team 2020). This method uses a PCA prior to the DA to infer genetic groups. The best-fit *K* cluster value was selected based on BIC following the tutorial (Jombart and Collins 2015). A NeighborNet phylogenetic network (Bryant and Moulton 2004) was inferred using SplitsTree v.4.14.2 (Huson and Bryant 2006) based on the genetic distance matrix among individuals calculated using TASSEL 5.2.66 (Bradbury et al. 2007). Furthermore, Jost's *D* was calculated for each population pair using GenAlEx v.6.501.

The direction and magnitude of gene flow among populations were estimated using the divMigrate function in the diveRsity package (Keenan et al. 2013) in R v.4.0.2 (R core team 2020). This program produces a migration network graph with relative values for gene flow among populations scaled to 1 at the largest magnitude estimated. Nei's G_{ST} was used as a measure of genetic differentiation. For the direction of gene flow between each population pair, the CIs were calculated by 1,000 bootstrap replicates, and overlap between the 95% CIs was evaluated.

Population demographic history

ABC methods implemented in DIYABC v.2.1 (Cornuet et al. 2014) were employed to infer the most likely demographic history of *E. bicyclis*. According to the above genetic structure assessments, Pp 4 was excluded owing to its highly mixed genetic cluster pattern. The remaining eight populations were classified into three regional population groups: Sea of Japan populations (Pop1: Ps 1–4), Eastern Pacific populations (Pop2: Pp 1–3), and Central Pacific population (Pop3: Pp 5). Completely missing loci within each population, as well as loci with minor allele frequencies < 0.01, were removed from the

246 original SNP dataset used for other population genetic analyses to meet the software
247 requirements.
248 In this ABC analysis, any population demographic scenarios are examinable.
249 However, since the validity is only inferred for a set of chosen scenarios, it is necessary
250 to test a wide number of possibilities to conduct a reliable analysis. Considering the
251 current distribution of this species, ocean currents, and the genetic structure detected
252 above, we first conducted preliminary ABC analyses with various scenarios. Based on
253 the preliminary ABC analyses, six demographic scenarios which include wide
254 possibilities were designed (Fig. 2). Scenarios 1 and 2 assume that Pop3 is the ancestor,
255 and differ in the order of divergence of the remaining two regional populations (Pop1
256 and Pop2). Scenario 3 assumes that Pop1 is ancestral and that the distribution expanded
257 geographically from the Pop1. Scenario 4 assumes that Pop2 is the ancestor and that the
258 distribution expanded in the opposite direction to that in scenario 3. In Scenario 5, Pop1
259 and Pop2 initially diverged across the Japanese archipelago, and then Pop3 was created
260 by secondary contact and hybridization. Finally, in scenario 6, all three regional
261 population groups diverged simultaneously, probably from an ancestral population that
262 had spread throughout the area around the Japanese archipelago. In developing these
263 scenarios, we did not account for the expansion of Pop1 or Pop2 through the Tsugaru
264 Strait (between Hokkaido and Honshu). This expansion is nearly impossible in terms of
265 ocean current flow and was not supported by our preliminary analyses. In these
266 scenarios, t# indicates time scale measured in generations (t1, t2, and t3), and N1–3 and
267 Na correspond to the effective population sizes for Pop1, Pop2, Pop3, and the ancestral
268 population, respectively. Scenario 5 included an admixture event wherein the admixture
269 rate ‘ra’ and ‘1-ra’ represent the genetic contribution of each ancestral population. In

this case, if ‘ra’ is close to 0, Pop3 mainly diverged from Pop2. Conversely, if ‘ra’ is close to 1, Pop3 mainly diverged from Pop1. Therefore, scenario 5 covers a wide range of possibilities. In scenario 6, a demographic event had occurred at a single point in t3; thus t1 and t2 have no meaning.

The parameter settings are listed in Table S2. We employed SS of genetic diversity and Nei’s distances for each population and each pair of populations, respectively. For both statistics, the proportion of zero values, variance of non-zero values, and mean of complete distribution were employed, for 18 SS in total. We simulated 1,000,000 datasets for each of the scenarios. To identify the most likely scenario, we compared the posterior probabilities of scenarios using both direct and logistic approaches. In the direct approach, the posterior probabilities of scenarios were estimated using the 500 simulated data closest to the observed data. A logistic regression with linear discriminant analysis on SS was applied for the logistic approach to estimate the posterior probabilities using 1% of simulated data showing the greatest similarity to the observed data. Confidence in the scenario choice was assessed using the DIYABC function ‘evaluate the confidence in scenario choice’ with logistic regression to estimate type I (false positives) and type II (false negative) errors with ‘linear discriminant analysis on SS’. Type I error is the probability of rejecting a scenario even though it is the true scenario, and type II error is the probability of selecting a scenario even though it is not the true scenario. To evaluate the error rates, we computed 1,000 datasets under all scenarios. We also used the option ‘model checking’ with PCA using DIYABC to assess the goodness of fit of the most likely scenario. This option can be used to evaluate the consistency of the observed data with the posterior predictive distribution of the model for the best scenario.

294

295 RESULTS

296 *General ddRAD-seq results*

297 We obtained 200,080,717 pairs of raw DNA sequences with an average of 2,273,645 ±
298 53,612 (mean ± SE) per sample. All raw ddRAD-seq reads were submitted to the DDBJ
299 Sequence Read Archive under accession number DRA012247–55 (Table S1). Following
300 the base call quality- and sequence length-based filtering and adapter trimming of the
301 R1 reads (see Materials and Methods), 53,368,014 reads (620,558 ± 51,504 per sample)
302 of 100 bp were obtained. After a Stacks analysis and subsequent SNP filtering, the final
303 dataset comprised 1,299 unlinked SNP loci for 76 *E. bicyclis* samples (Table S1). The
304 mean (min–max) genotyping rate for each individual was 78.6% (40.9–95.8%).

305

306 *Genetic diversity*

307 The estimated values for genetic diversity parameters and the fixation index are shown
308 in Table 1. Genetic diversity was higher in populations on the Pacific coast (Pp 1–5: *AR*
309 = 1.199, 1.078–1.325; *I* = 0.189, 0.104–0.259; and uH_E= 0.140, 0.08–0.200; mean, min–
310 max) than in populations in the Sea of Japan (Ps 1–4: *AR* = 0.947, 0.937–0.967; *I* =
311 0.024, 0.017–0.039; and uH_E = 0.017, 0.012–0.027). Among the Pacific coast
312 populations, genetic diversity was highest at the southern edge (Pp 5: Shimoda,
313 Shizuoka Prefecture) and lowest at the northern edge (Pp 1: Minami-sanriku, Miyagi
314 Prefecture). Diversity was consistently low in the Sea of Japan populations. N_p, a
315 measure of genetic uniqueness in each population, was also higher in populations on the
316 Pacific coast (N_P = 0.069, 0.005–0.189) than in those in the Sea of Japan (N_P = 0.012,
317 0.009–0.021). The fixation index was low and often negative in the Sea of Japan

318 populations but high and always positive in the Pacific Ocean populations (Table 1).
319 The contribution to allelic diversity (A_S, D_A, and A_T) was negative in all Sea of Japan
320 populations (Fig. 3). By contrast, except for D_A in Pp 1, all contributions were positive
321 in Pacific populations, with the highest values obtained for Pp 5 (Fig. 3).
322
323 *Genetic structure*
324 In the STRUCTURE analysis, the log-likelihood value LnP(K) increased gradually from
325 K = 1 to 4, and ΔK was highest for K = 2 and 3 (Fig. S1). Accordingly, we showed
326 results of K= 2 to 4 in Figure 1a. The results of 20 independent runs within K = 2, 3, and
327 4 were similar and stable, so that we evaluated the results with the highest log-
328 likelihood value among 20 runs for each K. The ΔK value was highest at K = 2, and the
329 genetic clusters clearly separated the populations in the Sea of Japan (Ps 1–4) and on the
330 Pacific coast (Pp 1–5). In the Central Pacific coast populations (Pp 4 and Pp 5), the Sea
331 of Japan cluster (yellow, gray in black and white version) was mixed with the Pacific
332 coast cluster (blue, off white in black and white version) at a relatively low frequency
333 (Fig. 1a, b). Low genetic diversity (H_E) and high genetic drift (F_{ST}) were detected in the
334 Sea of Japan cluster, whereas the opposite results were obtained for the Pacific coast
335 cluster (Fig. 1b). The ΔK value was second highest at K = 3, with a new genetic cluster
336 involving populations on the southern edge of the Pacific coast (Pp 5), in addition to the
337 clusters found at K = 2 associated with the Sea of Japan (Ps 1–4) and the Eastern Pacific
338 coast (Pp 1–3). For Pp 4, the assignment probabilities to the three clusters were mixed
339 (Fig. 1b). Similar to the results for K = 2, relatively low H_E and high F_{ST} values were
340 detected in the Sea of Japan cluster. Furthermore, Pp 4 and Pp 5 were assigned to
341 different clusters when K = 4 (Fig. 1a).

342 In the DAPC analysis, we retained 10 PCs, accounting for 68.97% of the total
343 variance. The BIC values indicated four to seven genetic clusters. At $K = 4$, individuals
344 were classified into four regional groups: Sea of Japan coast (Ps 1–4), Eastern Pacific
345 coast (Pp 1–3), Central Pacific coast (right five individuals from Pp 5 in Fig. 1a), and
346 Central Pacific coast (Pp 4 and rest of two individuals from Pp 5 in Fig. 1a; Fig. 4). The
347 individuals assigned to the last group corresponded to the individuals assigned to mixed
348 clusters at $K = 3$ and light green (light gray in black and white version) cluster at $K = 4$
349 in the STRUCTURE analysis (Fig. 1a). When the number of genetic clusters was five to
350 seven, the clusters were further divided based on four clusters (Fig. S2). Therefore, we
351 selected the result at $K = 4$.
352 The NeighborNet analysis showed four genetic clades: Sea of Japan populations (Ps
353 1–4), Eastern Pacific populations (Pp 1–3), and Central Pacific (Pp 4 and Pp 5) (Fig. 5).
354 Pp 4 was geographically located between Pp 5 and the Eastern Pacific populations (Pp
355 1, 2, and 3), and was genetically intermediate to these populations in the NeighborNet
356 analysis.
357 In the analysis of genetic differentiation (Jost's D) among all population pairs, while
358 inter-population differentiation within the Sea of Japan area was low for all population
359 pairs, levels of differentiation within the Pacific Ocean area were high (Fig. 6). In
360 particular, the Eastern Pacific population (Pp 1–3) and the southern edge of Central
361 Pacific population (Pp 5) showed high genetic differentiation (Jost's $D = 0.257–0.355$).
362 Gene flow estimates are shown in Fig. 7. Relatively high levels of gene flow were
363 mainly detected between populations within the Pacific coast (Pp 1–3) and the Sea of
364 Japan coast (Ps 1–4) (Fig. 7). Conversely, no substantial gene flow was detected
365 between the two coastal regions, except for weak gene flow from Ps 1 to Pp 5. Weak

366 gene flow into the Central Pacific populations (Pp 4 and Pp 5) from the Eastern Pacific
367 populations (Pp 1, 2, and 3) was detected. Bootstrap simulations showed significant
368 directional gene flow in the direction of influx from the surrounding populations (Ps 1
369 and 4) into Ps 2 in the Sea of Japan. Significant directional gene flow was also detected
370 in Ps 3 to Ps 2, although the magnitude of gene flow (0.29) was lower than our setting
371 of the threshold (0.30).
372
373 *Inference of population demographic history*
374 After additional SNP filtering, a dataset containing 1,002 SNP loci for 68 individuals
375 from eight populations was used for this DIYABC analysis. Among the six scenarios
376 (Fig. 2), the posterior probability was higher for scenario 6 (direct approach: 0.4400
377 with 0.0049–0.8751 of 95% CI, logistic approach: 0.9955 with 0.9942–0.9967 of 95%
378 CI) than for scenario 1 (0.1420, 95% CI: 0.0000–0.4480 and 0.0000, 95% CI: 0.0000–
379 0.0000), scenario 2 (0.2860. 95% CI: 0.0000–0.6821 and 0.0041, 95% CI: 0.0029–
380 0.0053), scenario 3 (0.0100. 95% CI: 0.0000–0.0972 and 0.0000, 95% CI: 0.0000–
381 0.0000), scenario 4 (0.1220. 95% CI: 0.0000–0.4089 and 0.0004, 95% CI: 0.0003–
382 0.0005), and scenario 5 (0.0000. 95% CI: 0.0000–0.0000 and 0.0000, 95% CI: 0.0000–
383 0.0000). As a result of model checking for scenario 6, the observed data were highly
384 similar to the simulated data in a PCA (Fig. S3). The probability of a type I error for
385 scenario 6 was $p = 0.2391$. The type II errors for scenario 6 under scenarios 1, 2, 3, and
386 4 were $p = 0.2078$, $p = 0.1753$, $p = 0.2857$, and $p = 0.1947$, respectively. For scenario 6,
387 the original mode values of t1, t2, and t3 were 373 (95% CI: 375–38,300), 34,900 (95%
388 CI: 5,580–51,100), and 45,900 (95% CI: 24,600–60,000) generations, respectively
389 (Table S3). The original modes of the effective population sizes N1, N2, N3, and Na

were 9,730 (95% CI: 4,570–14,100), 36,300 (95% CI: 22,800–45,100), 45,900 (95% CI: 18,400–49,500), and 146,000 (95% CI =129,000–150,000), respectively (Table S3). The generation time for *E. bicyclis* is roughly 3–6 years based on an ecological study (Taniguchi and Kito 1988, Kawamata 2012). Using this estimate, the meaningful divergence time in scenario 6 (t3) was converted to 137,700–275,400 years ago.

DISCUSSION

In the present study, we revealed the genetic structure of a canopy-forming kelp, *E. bicyclis*, using 1,299 genome-wide SNP loci. According to simulation studies (Haasl et al. 2011, Nazareno et al. 2017) and other recent phylogeographic studies using ddRAD-seq (Lu et al. 2020, Yoichi et al. 2021), the number of SNP markers and the sample size within populations in the present study would be sufficient for the phylogeographic analyses. By a combination of STRUCTURE, DAPC, and NeighborNet analyses, we detected four genetic groups distributed on the Eastern Pacific coast (Pp 1–3), Central Pacific coast (Pp 4), Central Pacific coast (Pp 5), and Sea of Japan coast (Ps 1–4). However, based on a STRUCTURE analysis assuming $K = 3$, Jost's D values, and relative gene flow, Pp 4 was in a transition zone between the groups on the Eastern Pacific coast (Pp 1–3) and Central Pacific coast (Pp 5), indicating that Pp 4 is a hybrid population. Therefore, this kelp is likely composed of three genetically distinct groups distributed on the Sea of Japan coast (Ps 1–4), Eastern Pacific coast (Pp 1–3), and Central Pacific coast (Pp 5). Similar to results of previous phylogeographic studies of brown algae in Japan (Uwai et al. 2006, Uwai 2010, Horiuchi et al. 2017, Kobayashi et al. 2018), the genetic boundary between the Eastern Pacific population and Central Pacific population of this kelp was identified as the area from the southern Tohoku to

414 Kanto regions.

415 The three genetic groups that distribute in different geographic regions suggested that
416 a distinct refugium existed in each of the three regions during LGM. Each of them
417 would have become the origin of the current three genetic groups, respectively. High,
418 intermediate, and low genetic diversity were detected in the Central Pacific, Eastern
419 Pacific, and Sea of Japan, respectively. These different patterns of genetic diversity
420 indicate heterogeneity in the demographic history of the three groups. Additionally, the
421 DIYABC analysis suggested the simultaneous split of the three groups in the greater
422 ancestral period (137,700–275,400 years ago), before the LGM. After divergence, large,
423 medium, and small effective population sizes were detected in the Central Pacific,
424 Eastern Pacific, and Sea of Japan, respectively. This pattern corresponds to the pattern
425 of genetic diversity described above. Thus, the three clusters were presumably
426 influenced differently by past geographic and climatic events.

427 Low genetic diversity and small effective population sizes were detected in *E.*
428 *bicyclis* in the Sea of Japan. These results suggest that the Sea of Japan populations
429 underwent severe bottlenecks in the past (e.g., during the LGM). Therefore, the present
430 wide distribution along the Sea of Japan coast probably formed after the LGM by a
431 rapid range expansion from refugia along the coast, supported by the high genetic
432 homogeneity in the Sea of Japan populations. A recent range expansion has also been
433 reported in *Cystoseira tamariscifolia* (Hudson) Papenfuss in northern Europe (Bermejo
434 et al. 2018) and *Laminaria digitata* (Hudson) J.V. Lamouroux in the Northeast Atlantic
435 (Neiva et al. 2020). During the LGM, in addition to cold water temperatures similar to
436 current temperatures in the northern Sea of Japan of 46–48°N, low salinity (26–29‰)
437 has been reported in the southern region of the Sea of Japan (Oba and Tanimura 2012).

438 Although studies of salinity tolerance are lacking in *E. bicyclis* and a few even in the
439 other kelp species, in general, kelp species can grow the salinity range of 26–29‰
440 (Bartsch et al. 2008). Water temperature in the past 5 years ranged from 6 to 21ºC in the
441 northernmost region of this kelp distribution (available here:
442 https://www.suigi.pref.iwate.jp/teichi, recorded in the depth of 3 m), and between 4 to
443 21 ºC in the northern Sea of Japan 46-48 ºN (available here: https://www.jma-
444 net.go.jp/sapporo/kaiyou/engan/engan.html, recorded at surface). Given this kelp can
445 survive ~ 5 ˚C (Kurashima et al. 1996), *E. bicyclis* could survive in the lower
446 temperature of the northern Sea of Japan 46-48 ºN. Accordingly, this kelp species has
447 the potential to survive in a wide area on the Sea of Japan coast, even during the LGM,
448 from this physiological perspective. Therefore, abiotic factors other than temperature
449 and salinity probably limited the distribution of *E. bicyclis* to refugia during the LGM.
450 For example, the kelp prefers strong light intensity, thereby limiting it to shallow water,
451 usually < 10 m in depth (Maegawa et al. 1988, Kurashima et al. 1996). It is possible that
452 photosynthetically active radiation could be a limiting factor in the past distribution of
453 this kelp, as the kelp is currently absent in coastal areas with heavy snowfall (i.e.,
454 frequently cloudy in the winter) in the Sea of Japan from Fukui Prefecture to Hokkaido.
455 In contrast to *E. bicyclis*, the Sea of Japan populations of *Sargassum thunbergii*
456 (Mertens ex Roth) Kuntze, an intertidal-dominant brown alga, show high genetic
457 diversity and large effective population sizes, suggesting their stable persistence in this
458 area (Kobayashi et al. 2018). More studies are needed to reveal the macroalgal
459 distribution in the Sea of Japan during the LGM.
460 The highest genetic diversity was detected in a *E. bicyclis* population at the southern
461 edge of the Pacific coast. In Japan, the highest genetic diversity was found in southern

462 populations in various species of brown algae, including *Sargassum fusiforme* (Harvey)
463 Setchell (Horiuchi et al. 2017) and *S. thunbergii* (Kobayashi et al. 2018), and in a red
464 alga, *Gelidium elegans* Kützing (Chimura et al. 2020). A similar pattern has been
465 reported for brown algae distributing European coasts, at localities considered to be
466 refugia during the LGM (Assis et al. 2014, 2016, Neiva et al. 2014, Bermejo et al. 2018,
467 Neiva et al. 2020, Schoenrock et al. 2020). Accordingly, the southern edge population of
468 *E. bicyclis* was probably maintained for a long time before the LGM. Given the
469 difference in genetic diversity between the Eastern and Central Pacific coasts, the
470 population size of *E. bicyclis* during the LGM was likely smaller on the Eastern Pacific
471 coast, as supported by the DIYABC.
472 Currently, many kelp forests are threatened by ocean warming (Kumagai et al. 2018,
473 Wernberg et al. 2019). Especially on temperate coasts, tropicalization increases kelp
474 consumption by herbivorous fish, and the decline or disappearance of kelps has been
475 found in various transition zones between temperate and tropical areas (Vergés et al.
476 2016, Zarco-Perello et al. 2017). In Japan, SST has risen by +1.16°C over the last 100
477 years (Japan Meteorological Agency:
478 https://www.data.jma.go.jp/gmd/kaiyou/english/long_term_sst_japan/sea_surface_temp
479 erature_around_japan.html). Declines in distribution within next 2-3 decades were
480 predicted for most kelp species in Japan (Kumagai et al. 2018, Sudo et al. 2020). As to
481 *E. bicyclis*, it has been predicted that southern central Pacific and southern Sea of Japan
482 population are highly vulnerable to heat stress and herbivorous feeding in 2009-2035
483 (Kumagai et al. 2018). Indeed, a long-term monitoring in northwestern Kyushu revealed
484 that losses of ecklonian kelp forests were driven by high temperature in summer,
485 subsequent feeding by herbivorous fish in autumn, and small number of recruitments

(Kiyomoto et al. 2021). Several studies have revealed the importance of potential deep sea refugia for temperate kelp against the global warming (Graham et al. 2007, Assis et al. 2016). However, *E. bicyclis* prefers a strong light intensity (Maegawa et al. 1988, Kurashima et al. 1996) and is therefore found in shallow water, usually at depths of < 10 m (Maegawa 1990, Sakanishi et al. 2018). Thus, deep sea refugia would be unavailable for this kelp.

E. bicyclis conservation efforts need to consider the genetic structure and genetic diversity revealed in the present study. The decline of *E. bicyclis* beds on the southern edge of the Pacific coast has recently been found at a long-term monitoring site (Biodiversity Center of Japan, Ministry of the Environment, Government of Japan 2020; http://www.biodic.go.jp/moni1000/index.html, Terada et al. 2020). In the present study, the southern populations in the Central Pacific (Pp 4 and Pp 5) contributed substantially to the total genetic diversity of this species. Therefore, the loss of Central Pacific populations (Pp 4 and Pp 5) would drastically decrease total genetic diversity within this kelp. Especially for our southern edge population, Pp 5, which showed the highest genetic diversity and the highest genetic uniqueness (Table 1), is only 3 km from this monitoring site and may be declining as well. Pp 5 also showed the highest F_{IS} values (Table 1), suggesting high level of inbreeding, probably as a result of the population decline. Similar to this kelp, high F_{IS} values in declining populations have been reported in *Saccorhiza polyschides* (Lightfoot) Batters (Assis et al. 2013). Inbreeding depression is frequently observed in animals and land plants (Frankham et al. 2002). It has not been a major concern in macroalgae but should be considered, in addition to genetic diversity and uniqueness. However, in a laminarialean kelp *Postelsia palmaeformis* Ruprecht, selfing did not reduce the fitness of the offspring (Barner et al. 2011), and further, in

small populations, the demographic processes had an affect greater than genetic diversity (Wootton and Pfister 2013). On the other hand, temporary drastic losses of *E. bicyclis* beds have been observed in the southern part of the Sea of Japan due to heat wave occurred in 2013 (Yatsuya 2014, Yoshida 2016). As revealed in the present study, all Sea of Japan populations have low genetic diversity, indicating that they may be vulnerable to environmental changes, such as climate change and feeding increases. Therefore, these populations need to be monitored for potentially rapid changes in response to environmental changes. Because the Sea of Japan populations formed a unique genetic cluster distinct from the Eastern and Central Pacific populations, their conservation is essential as well. Furthermore, future losses of southern populations in both the Central Pacific and Sea of Japan due to increased kelp consumption by herbivorous fish are predicted (Kumagai et al. 2018). Immediate conservation actions on the Central Pacific coast and southern Sea of Japan coast are needed to maintain *E. bicyclis* beds based on current genetic diversity levels. In addition, generally, a greater understanding of the effects of inbreeding and the loss of genetic diversity is needed across kelp species.

CONCLUSION

We revealed the genetic structure of a canopy-forming kelp, *E. bicyclis*, using genome-wide SNP loci in the present study. Three genetically distinct groups were detected in the Eastern Pacific, Central Pacific, and Sea of Japan. The estimated divergence time of these three groups was before the last glacial period. They likely survived for a long time after divergence in each region. The Central Pacific populations have high genetic diversity and uniqueness. The southern population in the Sea of Japan may be

vulnerable to environmental change due to its low genetic diversity. The conservation of *E. bicyclis* populations in these two areas is an urgent issue. The demonstrated effectiveness of reforestation of brown algae, inclusive of genetic considerations (Wood et al. 2020), emphasizes that phylogeographic studies like the present study, which can provide us fundamental genetic basis, have become more important. Phylogeographic studies on various canopy-forming brown algae are needed to effectively promote the conservation of macroalgal forests.

ACKNOWLEDGMENTS

We thank Dr. Mahiko Abe, Mr. Masayuki Fukuoka, Mr. Tetsuya Mukai, Dr. Noboru Murase, and Dr. Hiromori Shimabukuro (alphabetical order) for sample collection. This study was supported by the Waterfront Vitalization and Environment Research Foundation (W01108 to SS).

REFERENCES

Assis, J., Coelho, N. C., Alberto, F., Valero, M., Raimondi, P., Reed, D. & Serrão, E. Á. 2013. High and distinct range-edge genetic diversity despite local bottlenecks. *PLoS One* 8:68646.

Assis, J., Coelho, N. C., Lamy, T., Valero, M., Alberto, F. & Serrão, E. Á. 2016. Deep reefs are climatic refugia for genetic diversity of marine forests. *J. Biogeogr.* 43:833–44.

Assis, J., Serrão, E. Á., Claro, B., Perrin, C. & Pearson, A. G. 2014. Climate-driven

range shifts explain the distribution of extant gene pools and predict future loss of unique lineages in a marine brown alga. *Mol. Ecol*. 23:2797–810.

Avise, J. C. 2000. *Phylogeography: The History and Formation of Species.* Harvard University Press, Cambridge.

Baba, M. 2010. Effects of temperature and irradiance on the growth of gametophyte and young sporophyte of *Eisenia bicyclis* in laboratory culture. *Rep. Mar. Ecol. Res. Inst.* 13:75–82. (in Japanese with English abstract)

Baba, M. 2021. Growth responses and distributional changes of large brown seaweeds due to global warming *Rep. Mar. Ecol. Res. Inst.* 26:1–28. (in Japanese with English abstract)

Barner, A. K., Pfister, C. A. & Wootton, J. T. 2011. The mixed mating system of the sea palm kelp *Postelsia palmaeformis*: few costs to selfing. *Proc. R. Soc. B.* 278:1347–55.

Bartsch, I., Wiencke, C., Bischof, K., Cornelia, M. B., Buck, H. B., Eggert, A., Feuerpfeil, P., Hanelt, D., Jacobsen, S., Karez, R., Karsten, U., Molis, M., Roleda, M. Y., Schubert, H., Schumann, R., Valentin, K., Weinberger, F. & Wiese, J. 2008. The genus *Laminaria* sensu lato: recent insights and developments. *Europ. J. Phycol.* 43:1–86.

582 Bermejo, R., Chefaoui, R. M., Engelen, A. H., Buonomo, R., Neiva, J., Ferreira-Costa,
583 J., Pearson, G. A., Marbà, N., M. Duarte, C. M., Airoldi, L., Hernández, I., Guiry,
584 M. D. & Serrão, E. Á . 2018. Marine forests of the Mediterranean-Atlantic
585 *Cystoseira tamariscifolia* complex show a southern Iberian genetic hotspot and no
586 reproductive isolation in parapatry. *Sci. Rep.* 8:10427.
587
588 Bradbury P. J., Zhang Z., Kroon D. E., Casstevens, T. M., Ramdoss, Y. & Buckler, E. S.
589 2007. TASSEL: software for association mapping of complex traits in diverse
590 samples. *Bioinformatics* 23:2633–5.
591
592 Bryant, D. & Moulton, V. 2004. Neighbor-net: an agglomerative method for the
593 construction of phylogenetic networks. *Mol. Biol. Evol.* 21:255–65.
594
595 Caballero, A., Rodríguez-Ramilo, S. T., Ávila, V. & Fernández, J. 2010. Management of
596 genetic diversity of subdivided populations in conservation programmes. *Conserv.*
597 *Genet*. 11:409–19.
598
599 Catchen, J. M., Amores, A., Hohenlohe, P., Cresko, W. & Postlethwait, J. H.. 2011.
600 Stacks: building and genotyping loci de novo from short-read sequences. *G3*
601 *(Bethesda)* 1:171–82.
602
603 Chimura, K., Iwasaki, T., Akita, S. & Shimada, S. 2020. RAD-seq based
604 Phylogeographic study of *Gelidium elegans* (Rhodophyta) around Japanese coast.
605 *Algal Resour.* 20:117–20. (in Japanese with English abstract)

606

607 Chung, I. K., Oak, J. H., Lee, J. A., Shin, J. A., Kim, J. G. & Park, K. S. 2013. Installing
608 kelp forests/seaweed beds for mitigation and adaptation against global warming:
609 Korean Project Overview. *ICES J. Mar. Sci.* 70:1038–44.

610

611 Cornuet, J. M., Pudlo, P., Veyssier, J., Dehne-Garcia, A., Gautier, M., Leblois, R.,
612 Marin, J. M. & Estoup, A. 2014. DIYABC v.2. 0: a software to make approximate
613 Bayesian computation inferences about population history using single nucleotide
614 polymorphism, DNA sequence and microsatellite data. *Bioinformatics* 30:1187–9.

615

616 Doyle, J. J. & Doyle, J. L. 1990. Isolation of plant DNA from fresh tissue. *Focus.*
617 12:39–40.

618

619 Duforet-Frebourg, N., Bazin, E. & Blum, M. G. 2014. Genome scans for detecting
620 footprints of local adaptation using a Bayesian factor model. *Genome. Biol. Evol.*
621 31:2483–95.

622

623 Earl, D.A. & von Holdt, B.M. 2012. STRUCTURE HARVESTER: a website and
624 program for visualizing STRUCTURE output and implementing the Evanno
625 method. *Conserv. Gene. Resour.* 4:359–61.

626

627 Edwards, S. V., Shultz, A. J. & Campbell-Staton, S. C. 2015. Next-generation
628 sequencing and the expanding domain of phylogeography. *Folia Zool.* 64:187–206.

629

630 Evanno, G., Regnaut, S. & Goudet, J. 2005. Detecting the number of clusters of
631 individuals using the software STRUCTURE: A simulation study. *Mol. Ecol*.
632 14:2611–20.
633
634 Falush, D., Stephens, M. & Pritchard, J.K. 2003. Inference of population structure using
635 multilocus genotype data: linked loci and correlated allele frequencies. *Genetics.*
636 164:1567–87.
637
638 Filbee-Dexter, K. & Scheibling, R. E. 2014. Sea urchin barrens as alternative stable
639 states of collapsed kelp ecosystems. *Mar. Ecol. Prog. Ser.* 495:1–25.
640
641 Frankham, R., Ballou, S. E. J. D., Briscoe, D. A. & Ballou, J. D. 2002. Introduction to
642 conservation genetics. Cambridge university press.
643
644 Fredriksen, S., Filbee-Dexter, K., Norderhaug, K. M., Steen, H., Bodvin, T., Coleman,
645 M. A., Moy, F. & Wernberg, T. 2020. Green gravel: a novel restoration tool to
646 combat kelp forest decline. *Sci. Rep.* 10:3983.
647
648 Fujita, D. 2010. Current status and problems of isoyake in Japan. *Bull. Fish. Res. Agen.*
649 32: 33–42.
650
651 Gianni, F., Bartolini, F., Pey, A. Laurent, M., Martins, G. M., Airoldi, L. & Mangialajo,
652 L. 2017. Threats to large brown algal forests in temperate seas: the overlooked role
653 of native herbivorous fish. *Sci. Rep.* 7:6012.

654

655 Graham, M. H. 2004. Effects of local deforestation on the diversity and structure of
656 southern California giant kelp forest food webs. *Ecosystems* 7:341–57.

657

658 Graham, M. H., Kinlan, B. P., Druehl, L. D., Garske, L. E. & Banks, S. 2007. Deep-
659 water kelp refugia as potential hotspots of tropical marine diversity and
660 productivity. *Proc. Natl. Acad. Sci. USA* 104:16576–80.

661

662 Guzinski, J., Ballenghien, M., Daguin-Thiébaut, C., Lévêque, L. & Viard, F. 2018.
663 Population genomics of the introduced and cultivated Pacific kelp *Undaria*
664 *pinnatifida*: Marinas−not farms−drive regional connectivity and establishment in
665 natural rocky reefs. *Evol. Appl.* 11:1582–97.

666

667 Haasl, R. J. & Payseur, B. A. 2011. Multi-locus inference of population structure: a
668 comparison between single nucleotide polymorphisms and microsatellites.
669 *Heredity.* 106:158-71.

670

671 Hoban, S, Bruford, M., D'Urban Jackson, J. Lopes-Fernandes, M., Heuertz, M.,
672 Hohenlohe, P. A., Paz-Vinas, I., Sjögren-Gulve, P., Segelbacher, G., Vernesi, C.,
673 Aitken, S., Bertola, L. D., Bloomer, P., Breed, M., Rodríguez-Correa, H., Funk, W.
674 C., Grueber, C. E., Hunter, M. E., Jaffe, R., Liggins, L., Mergeay, J., Moharrek, F.,
675 O'Brien, D., Ogden, R., Palma-Silva, C., Pierson, J., Ramakrishnan, U., Simo-
676 Droissart, M., Tani, N., Waits, L. & Laikre, L. 2020. Genetic diversity targets and

677 indicators in the CBD post-2020 Global Biodiversity Framework must be
678 improved. *Biol. Conserv.* 248:108654.
679
680 Horiuchi H, Kobayashi, H., Iwasaki, T. & Shimada, S. 2017. Phylogeograchic analyses
681 of *Sargrassum fusiforme* (Sargassaceae, Phaeophyceae) distributed around
682 Japanese coast. *Jpn. J. Phycol. (Sôrui)* 65:139–48.
683
684 Hu, Z. M., Duan, D. L. & Lopez-Bautista, J. 2016. Seaweed phylogeography from 1994
685 to 2014: an overview. *In* Hu, Z. M. & Fraser, C. [Eds.] *Seaweed phylogeography*.
686 Springer, Dordrecht, pp. 3–22.
687
688 Hughes, A. R. & Stachowicz, J. J. 2004. Genetic diversity enhances the resistance of a
689 seagrass ecosystem to disturbance. *Proc. Natl. Acad. Sci. USA* 101:8998–9002.
690
691 Huson, D. H. & Bryant, D. 2006. Application of phylogenetic networks in evolutionary
692 studies. *Mol. Biol. Evol.* 23:254–67.
693
694 Jombart, T. & Ahmed, I. 2011. Adegenet 1.3-1: new tools for the analysis of genome-
695 wide SNP data. *Bioinformatics* 27:3070–1.
696
697 Jombart, T. & Collins, C. 2015. A tutorial for discriminant analysis of principal
698 components (DAPC) using adegenet 2.0.0. available here: https://adegenet.r-
699 forge.r-project.org/files/tutorial-dapc.pdf
700

701 Jombart, T., Devillard, S. & Balloux, F. 2010. Discriminant analysis of principal
702 components: a new method for the analysis of genetically structured populations.
703 *BMC Genetics* 11:94.
704
705 Kai, W., Nomura, K., Fujiwara, A., Nakamura, Y., Yasuike, M., Ojima, N., Masaoka, T.,
706 Ozaki, A., Kazeto, Y., Gen, K., Nagao, J., Tanaka, H., Kobayashi, T. & Ototake, M.
707 2014. A ddRAD-based genetic map and its integration with the genome assembly
708 of Japanese eel (*Anguilla japonica*) provides insights into genome evolution after
709 the teleost-specific genome duplication. *BMC Genomics* 15:1–16.
710
711 Kawai, H., Akita S., Hashimoto K. & Hanyuda T. 2020. A multigene molecular
712 phylogeny of *Eisenia* reveals evidence for a new species, *Eisenia nipponica*
713 (Laminariales), from Japan. *Europ. J. Phycol*. 55:234–41.
714
715 Kawamata, S. 2012. Use of beached plants to analyze the allometry, modes of failure
716 and life time of the kelp *Eisenia bicyclis*. *Jpn. J. Phycol (Sorui)* 60:127–30. (in
717 Japanese with English abstract)
718
719 Keenan, K., McGinnity, P., Cross, T. F., Crozier, W. W. & Prodöhl, P. A.. 2013.
720 diveRsity: an R package for the estimation and exploration of population genetics
721 parameters and their associated errors. *Met. Ecol. Evol.* 4:782–8.
722
723 Kiyomoto, S., Yamanaka, H., Yoshimura, T., Yatsuya, K., Shao, H., Kadota, T. &
724 Tamaki, A. 2021. Long-term change and disappearance of Lessoniaceae marine

725 forests off Waka, Ikishima Island, northwestern Kyushu, Japan. *Nippon Suisan*
726 *Gakkaishi* Advanced online publication, DOI: 10.2331/suisan.21-00013. (in
727 Japanese with English abstract)
728
729 Kobayashi, H., Haino, Y., Iwasaki, T., Tezuka, A., Nagano, A. J. & Shimada, S. 2018.
730 ddRAD-seq based phylogeographic study of *Sargassum thunbergii* (Phaeophyceae,
731 Heterokonta) around Japanese coast. *Mar. Environ. Res.* 140:104–13.
732
733 Krause-Jensen, D. & Duarte, C. M. 2016. Substantial role of macroalgae in marine
734 carbon sequestration. *Nature Geoscience* 9:737–42.
735
736 Krumhansl, K. A., Okamoto, D. K., Rassweiler, A., Novak, M., Bolton, J. J.,
737 Cavanaugh, K. C., Connell, S. D., Johnson, C. R., Konar, B., Ling, S. D., Micheli,
738 F., Norderhaug, K. M., Pérez-Matus, A., Sousa-Pinto, I., Reed, D. C., Salomon, A.
739 K., Shears, N. T., Wernberg, T., Anderson, R. J., Barrett, N. S., Buschmann, A. H.,
740 Carr, M. H., Caselle, J. E., Derrien-Courtel, S., Edgar, G. J., Edwards, M., Estes, J.
741 A., Goodwin, C., Kenner, M. C., Kushner, D. J., Moy, F. E., Nunn, J., Steneck, R.
742 S., Vásquez, J., Watson, J., Witman, J. D. & Byrnes, J. E. K. 2016. Global patterns
743 of kelp forest change over the past half-century. *Proc. Natl Acad. Sci.* 113:13785–
744 90.
745
746 Kumagai, N. H., Molinos, J. G., Yamano, H., Takao, S., Fujii, M. & Yamanaka, Y. 2018.
747 Ocean currents and herbivory drive macroalgae-to-coral community shift under
748 climate warming. *Proc. Natl. Acad. Sci.* 115:8990–5.

Kurashima, A., Yokohama, Y. & Aruga, A. 1996. Physiological characteristics of *Eisenia bicyclis* Setchell and *Ecklonia cava* Kjellman (Phaeophyta). *Jpn. J. Phyco.l (Sorui)* 44:87–94. (in Japanese with English abstract)

Le Cam, S., Daguin-Thiébaut, C., Bouchemousse, S., Engelen, A. H., Mieszkowska, N. & Viard, F. 2020. A genome-wide investigation of the worldwide invader *Sargassum muticum* shows high success albeit (almost) no genetic diversity. *Evol. Appl.* 13:500–14.

Ling, S. D., Ibbott, S. & Sanderson, J. C. 2010. Recovery of canopy-forming macroalgae following removal of the enigmatic grazing sea urchin *Heliocidaris erythrogramma*. *J. Exp. Mar. Biol. Ecol.* 395:135–46.

Ling, S. D., Scheibling, R. E., Rassweiler, A., Johnson, C. R., Shears, N., Connell, S. D., Salomon, A. K., Norderhaug, K. M., Pérez-Matus, A., Hernández, J. C., Clemente S., Blamey, L. K., Hereu, B., Ballesteros, E., Sala, E., Garrabou, J., Cebrian, E., Zabala M., Fujita, D. & Johnson, L. E. 2015. Global regime shift dynamics of catastrophic sea urchin overgrazing. *Phil. Trans. R. Soc. B* 370:20130269.

López-Cortegano, E., Pérez-Figueroa, A. & Caballero, A. 2019. metapop2: Re-implementation of software for the analysis and management of subdivided populations using gene and allelic diversity. *Mol. Ecol. Resour.* 19:1095–100.

773 Lu, R. S., Chen, Y., Tamaki, I., Sakaguchi, S., Ding, Y. Q., Takahashi, D., Li, P., Isaji, Y.,
774 Chen, J. & Qiu, Y. X. 2020. Pre-quaternary diversification and glacial demographic
775 expansions of *Cardiocrinum* (Liliaceae) in temperate forest biomes of Sino-
776 Japanese Floristic Region. *Mol. Phylogenet. Evol.* 143:106693.
777
778 Maegawa, M. 1990. Ecological studies of *Eisenia bicyclis* (KJELLMA) SETCHELL
779 and *Ecklonia cava* KJELLMAN. *Bull. Fac. Bioresources. Mie Univ*. 4:73–145.
780
781 Maegawa, M., Kida, W., Yokohama, Y. & Aruga Y. 1988. Comparative studies on
782 critical light conditions for young *Eisenia bicyclis* and *Ecklonia cava*. *Jpn. J.*
783 *Phycol. (Sorui)* 36:166–74.
784
785 Martin, M. 2011. Cutadapt removes adapter sequences from high-throughput
786 sequencing reads. *EMBnet.journal* 17:10–2.
787
788 Miller, M. R., Dunham, J. P., Amores, A., Cresko, W. A. & Johnson, E. A. 2007. Rapid
789 and cost-effective polymorphism identification and genotyping using restriction
790 site associated DNA (RAD) markers. *Genome Res.* 17:240–8.
791
792 Moritz, C. 2002. Strategies to Protect Biological Diversity and the Evolutionary
793 Processes That Sustain It. *Syst. Biol.* 51:238–54.
794
795 Nazareno, A. G., Bemmels, J. B., Dick, C. W. & Lohmann, L. G. 2017. Minimum
796 sample sizes for population genomics: an empirical study from an Amazonian plant

797 species. *Mol. Ecol. Resour.* 17:1136–47.
798
799 Neiva, J., Assis, J., Fernandes, F., Pearson, G. A., & Serrao, E. Á. 2014. Species
800 distribution models and mitochondrial DNA phylogeography suggest an extensive
801 biogeographical shift in the high-intertidal seaweed *Pelvetia canaliculata*. *J.*
802 *Biogeogr.* 41:1137–48.
803
804 Neiva, J., Serrão, E. Á., Paulino, C., Gouveia, L., Want, A., Tamigneaux, É.,
805 Ballenghien, M., Mauger, S., Fouqueau, L., Engel-Gautier, C., Destombe, C. &
806 Valero, M. 2020. Genetic structure of amphi-Atlantic *Laminaria digitata*
807 (Laminariales, Phaeophyceae) reveals a unique range-edge gene pool and suggests
808 post-glacial colonization of the NW Atlantic. *Europ. J. Phycol.* 55:517–28.
809
810 North, W. J. 1971. The biology of giant kelp beds (*Macrocystis*) in California:
811 introduction and background. *Nova Hedwigia* 32:1–68.
812
813 Oba, T. & Tanimura, Y. 2012. Surface environments in the Japan Sea around the last
814 glacial maximum. *Jour. Geol. Soc. Japan*. 118:376–86.
815
816 Ohta, M. 1988. Effects of water temperature on the growth and maturation of
817 gametophytes and on the growth of Juvenile sporophytes of *Eisenia bicyclis*
818 (Kjellman) Setchell and *Ecklonia cava* Kjellman (Phaeophyta, Laminariales). *Rep.*
819 *Mar. Ecol. Res. Inst.* 88202:1–29. (in Japanese with English abstract)
820

821 Ohtake, Y., Shimada, S. & Akita, S. 2020 High-temperature tolerance of a brown alga
822 *Eisenia bicyclis* collected from different localities. *Algal Resources* 13:85–9. (in
823 Japanese with English abstract)
824
825 Peakall, R. & Smouse, P.E. 2012. GenAlEx 6.5: genetic analysis in Excel. Population
826 genetic software for teaching and research-an update. *Bioinformatics* 28:2537–39.
827
828 Peterson, B. K., Weber, J. N., Kay, E. H., Fisher, H. S. & Hoekstra, H. E. 2012. Double
829 digest RADseq: an inexpensive method for de novo SNP discovery and genotyping
830 in model and non-model species. *PloS One* 7: e37135.
831
832 Pritchard, J. K., Stephens, M. & Donnelly, P. 2000. Inference of population on structure
833 using multilocus locus genotype data. *Genetics* 155: 945–59.
834
835 Pritchard, J. K., Wen, W. & Falush, D. 2010. Documentation for STRUCTURE
836 Software. version 2.3. available here: http://pritch.bsd.uchicago.edu/structure.html.
837
838 R Core Team 2020. R: A language and environment for statistical computing. R
839 Foundation for Statistical Computing, Vienna, Austria. URL https://www.R-
840 project.org/.
841
842 Rogers-Bennett, L. & Catton, C. A. 2019. Marine heat wave and multiple stressors tip
843 bull kelp forest to sea urchin barrens. *Sci. Rep*. 9:15050.
844

Sakanishi, Y., Kurashima, A., Dazai, A., Abe, T., Aoki, M. & Tanaka, J. 2018. Long-term changes in a kelp bed of *Eisenia bicyclis* (Kjellman) Setchell due to subsidence caused by the 2011 Great East Japan Earthquake in Shizugawa Bay, Japan. *Phycol. Res.* 66**:**253–61.

Schoenrock, K. M., O'Connor, A. M., Mauger, S., Valero, M., Neiva, J., Serrao, E. Á. & Krueger-Hadfield, S. A.. 2020. Genetic diversity of a marine foundation species, *Laminaria hyperborea* (Gunnerus) Foslie, along the coast of Ireland. *Europ. J. Phycol.* 55:310–26.

Steneck, R. S., Graham, M. H., Bourque, B. J., Corbett, D., Erlandson, J. M., Estes, J. A. & Tegner, M. J. 2002. Kelp forest ecosystems: biodiversity, stability, resilience and future. *Environ. Conser.* 29:436–59.

Steneck, R.S. & Johnson, C. 2014. Kelp forests: dynamic patterns, processes and feedbacks. *In* Bertness, M. D. Bruno, J. F., Silliman, B.R., Stachowicz, J. J. [Eds.] *Marine Community Ecology and Conservation*, Sinauer Associates, Sunderland, pp. 315–66.

Sudo, K., Watanabe, K., Yotsukura, N., & Nakaoka, M. 2020. Predictions of kelp distribution shifts along the northern coast of Japan. *Ecol. Res.* 35:47–60.

Tanaka, K., Ohno, M. & Largo, D. B. 2020. An update on the seaweed resources of Japan. *Bot. Mar.* 63:105–17.

Taniguchi, K. & Agatsuma, Y. 2001. Marine afforestation of the kelp *Eisenia bicyclis* in coralline flats. *Aquacult. Sci.* 49:133–6.

Taniguchi, K. & Kito, H. 1988. Age composition in the population of *Eisenia bicyclis* (Laminariaceae; Phaeophyta). *Nippon Suisan Gakkaishi* 54:1583–8. (in Japanese with English abstract)

Taniguchi, K., Yamane, H., Sasaki, K., Agatsuma, Y. & Arakawa, H. 2001. Marine afforestation of the kelp *Eisenia bicyclis* in coralline flats by introduction of porous-concrete reefs. *Nippon Suisan Gakkaishi* 67:858–65. (in Japanese with English abstract)

Terada, R., Abe, M., Abe, T., Aoki, M., Dazai, A., Endo, H., Kamiya, M., Kawai, H., Kurashima, A., Motomura, T., Murase, N., Sakanishi, Y., Shimabukuro, H., Tanaka, J., Yoshida, G. & Aoki, M. 2020. Japan's nationwide long-term monitoring survey of seaweed communities known as the “Monitoring Sites 1000”: Ten-year overview and future perspectives. *Phycol. Res.* 69:12–30.

Uwai, S., Nelson, W., Neill, K., Wang, W. D., Aguilar-Rosas, L. E., Boo, S. M., Kitayama, T. & Kawai, H. 2006. Genetic diversity in *Undaria pinnatifida* (Laminariales, Phaeophyceae) deduced from mitochondria genes–origins and succession of introduced populations. *Phycologia* 45:687–95.

893 Uwai, S., 2010. Geographic structure of seaweed populations on the Japanese coast.
894 *BSJ- Review* 1:57–65. (in Japanese)
895
896 Vergés, A., Doropoulos, C., Malcolm, H. A., Skye, M., Garcia-Pizá, M., Marzinelli, E.
897 M., Campbell, A. H., Ballesteros, E., Hoey, A. S., Vila-Concejo, A., Bozec, Y. M.
898 & Steinberg, P. D. 2016. Long-term empirical evidence of ocean warming leading
899 to tropicalization of fish communities, increased herbivory, and loss of kelp. *Proc.*
900 *Natl. Acad. Sci. USA* 113:13791–6.
901
902 Wernberg, T., Bennett, S. & Babcock, R. C. 2016. Climate-driven regime shift of a
903 temperate marine ecosystem. *Science* 353:169–72.
904
905 Wernberg, T., Coleman, M. A., Bennett, S., Thomsen, M. S., Tuya, F. & Kelaher, B. P.
906 2018. Genetic diversity and kelp forest vulnerability to climatic stress. *Sci. Rep*.
907 8:1851.
908
909 Wernberg, T., Krumhansl, K., Filbee-Dexter, K. & Pedersen, M. F. 2019. Status and
910 trends for the world's kelp forests. *In* Sheppard, C. [Ed] *World seas: an*
911 *environmental evaluation.* Academic Press, Cambridge, pp. 57–78.
912
913 Westermeier, R., Murúa, P., Patiño, D. J., Muñoz, L., Atero, C. & Müller, D. G. 2014.
914 Repopulation techniques for *Macrocystis integrifolia* (Phaeophyceae:
915 Laminariales) in Atacama, Chile. *J. Appl. Phycol*. 26:511–8.
916

917 Wood, G., Marzinelli, E. M., Vergés, A., Campbell, A. H., Steinberg, P. D. & Coleman,
918 M. A. 2020. Using genomics to design and evaluate the performance of underwater
919 forest restoration. *J. App. Ecol.* 57:1988–98.
920
921 Wootton, J.T., & Pfister, C.A. 2013. Experimental separation of genetic and
922 demographic factors on extinction risk in wild populations. *Ecology*. 94: 2117–23.
923
924 Yatsuya, K., Kiriyama, T., Kiyomoto, S., Taneda, T. & Yoshimura, T. 2014. On the
925 deterioration process of *Ecklonia* and *Eisenia* beds observed in 2013 at Gounoura,
926 Iki Island, Nagasaki Prefecture, Japan. Initiation of the bed degradation due to high
927 water temperature in summer and subsequent cascading effect by the grazing of
928 herbivorous fish in autumn. *Algal Resour* 7:79–94. (in Japanese with English
929 abstract)
930
931 Yoichi, W., Takahashi, M., Nagano, A. J., Uehara, K. & Abe, H. 2021. Evolutionary
932 effects of geographic and climatic isolation between *Rhododendron tsusiophyllum*
933 populations on the Izu Islands and mainland Honshu of Japan. *Heredity.* 126:859–
934 868.
935
936 Yoshida, D. 2016. The results of the interviews about the seaweed bed situation and
937 rocky-shore denudation in Coastal areas, Shimane Prefecture. *Rep. Shimane Pref.*
938 *Fish. Tech. Ctr.* 9:37–42. (in Japanese with English abstract)
939
940 Yotsui, T. & Maesako, N. 1993. Restoration experiments of *Eisenia bicyclis* beds on

941 barren grounds at Tsusima islands. *Aquacult. Sci.* 41:67–70. (in Japanese with
942 English abstract)
943
944 Zarco-Perello, S., Wernberg, T., Langlois, T. J. & Vanderklift, M. A. 2017.
945 Tropicalization strengthens consumer pressure on habitat-forming seaweeds. *Sci.*
946 *Rep.* 7:820.

947 **Table 1.** Genetic diversity of *Eisenia bicyclis* populations collected in the present study

Population code	N	N_A	N_E	N_P	*AR* [7]	*I*	H_O	H_E	uH_E	F_{IS}
Ps 1	9	1.030	1.013	0.009	0.939	0.019	0.017	0.013	0.013	-0.274
Ps 2	9	1.079	1.037	0.021	0.967	0.039	0.025	0.025	0.027	0.011
Ps 3	8	1.028	1.014	0.008	0.937	0.017	0.015	0.011	0.012	-0.182
Ps 4	8	1.039	1.024	0.010	0.945	0.022	0.02	0.014	0.016	-0.293
Pp 1	7	1.156	1.088	0.005	1.078	0.104	0.063	0.070	0.080	0.070
Pp 2	10	1.348	1.194	0.013	1.164	0.177	0.080	0.117	0.127	0.281
Pp 3	10	1.332	1.174	0.037	1.157	0.167	0.089	0.109	0.117	0.166
Pp 4	8	1.447	1.255	0.104	1.271	0.240	0.127	0.159	0.178	0.184
Pp 5	7	1.443	1.286	0.189	1.325	0.259	0.077	0.175	0.200	0.522
Mean	8.4	1.211	1.120	0.044	1.087	0.116	0.057	0.077	0.086	0.233

948 N = No. of specimens, N_A = No. of different alleles, N_E = No. of effective alleles, N_P = No. of private alleles, AR = Allelic richness (the
949 number in square brackets is the rarefaction size corresponding to the smallest sample size in the present study), I = Shannon's
950 information index, H_O = Observed heterozygosity, H_E = Expected heterozygosity, uH_E = Unbiased expected heterozygosity, F_{IS} =

951 fixation index.

FIGURE LEGENDS

Fig. 1. Distribution of *Eisenia bicyclis* (gray area), localities of collection sites (star), and genetic clustering based on a STRUCTURE analysis setting $K = 2$, $K = 3$, and $K = 4$. Each vertical bar shows the assignment probability for individuals (a). Pie charts in the map indicate the frequency of each cluster in the population (b).

Fig. 2. Six scenarios for the demographic histories of *Eisenia bicyclis* obtained using DIYABC v.2.1. t# represents the time scale measured in the number of generations. N1–3 and Na correspond to effective population sizes for Pop 1, Pop 2, Pop 3, and the ancestral population. The most likely scenario is shown by a double underline.

Fig. 3. Contributions of nine *Eisenia bicyclis* populations to overall genetic diversity and diversity within and between populations on the basis of allelic diversity.

Fig. 4. Discriminant analysis of principal components at $K = 4$ for the *Eisenia bicyclis* samples in the present study. Asterisks indicate individuals from Pp 5 within the Central Pacific cluster (Pp 4 and Pp 5).

Fig. 5. NeighborNet inferred using 76 samples from nine *Eisenia bicyclis* populations. Instead of sample IDs, population codes are indicated on the tips of branches.

Fig. 6. Pairwise genetic differentiation values (Jost's *D*) for all population pairs. The black-to-white gradient corresponds to the change from higher to lower values.

Fig. 7. Direction and relative magnitudes of gene flow among the nine *Eisenia bicyclis* populations. Relative gene flow estimates of < 0.30 are not shown. Asterisks (*) show significant directional gene flow based on 1,000 bootstrap replicates.

SUPPLEMENTARY FIGURES AND TABLES

Fig. S1. Delta *K* values (a) and LnP (*K*) (b) in each *K* cluster in a STRUCTURE analysis.

Fig. S2. BIC values for each value of *K* (a). Discriminant analysis of principal components for *K* = 5 (b), *K* = 6 (c), and *K* = 7 (d) based on *Eisenia bicyclis* collected in the present study.

Fig. S3. PCA of SS for the best-supported scenario 6 based on 1,000 simulations in the DIYABC analysis.

Table S1. Sample information includes the population code, locality, number of samples collected, and final dataset for analysis

Table S2. Prior distributions of the parameters used in DIYABC

Table S3. Original demographic parameters estimated by DIYABC in scenario 6

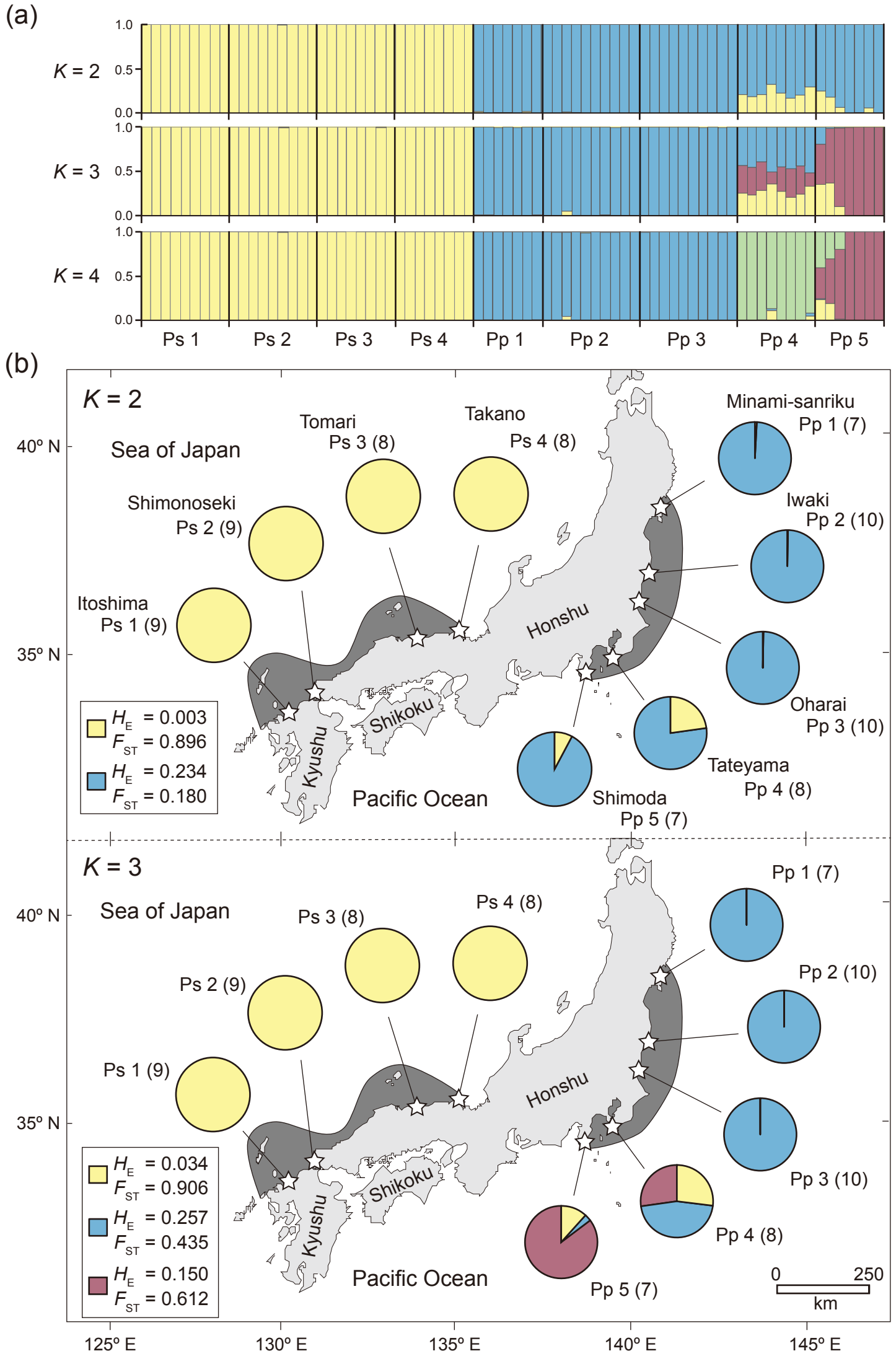
(a)
K = 2
K = 3
K = 4
1.0
0.5
0.0
Ps 1
Ps 2
Ps 3
Ps 4
Pp 1
Pp 2
Pp 3
Pp 4
Pp 5
(b)
K = 2
Sea of Japan
Tomari
Ps 3 (8)
Takano
Ps 4 (8)
Minami-sanriku
Pp 1 (7)
Shimonoseki
Ps 2 (9)
Iwaki
Pp 2 (10)
Itoshima
Ps 1 (9)
Honshu
Oharai
Pp 3 (10)
Shikoku
Kyushu
Tateyama
Pp 4 (8)
Pacific Ocean
Shimoda
Pp 5 (7)
H_E = 0.003
F_ST = 0.896
H_E = 0.234
F_ST = 0.180
40º N
35º N
K = 3
Sea of Japan
Ps 3 (8)
Ps 4 (8)
Pp 1 (7)
Ps 2 (9)
Pp 2 (10)
Ps 1 (9)
Honshu
Pp 3 (10)
Shikoku
Kyushu
Pp 4 (8)
Pacific Ocean
Pp 5 (7)
H_E = 0.034
F_ST = 0.906
H_E = 0.257
F_ST = 0.435
H_E = 0.150
F_ST = 0.612
0
250
km
125º E
130º E
135º E
140º E
145º E

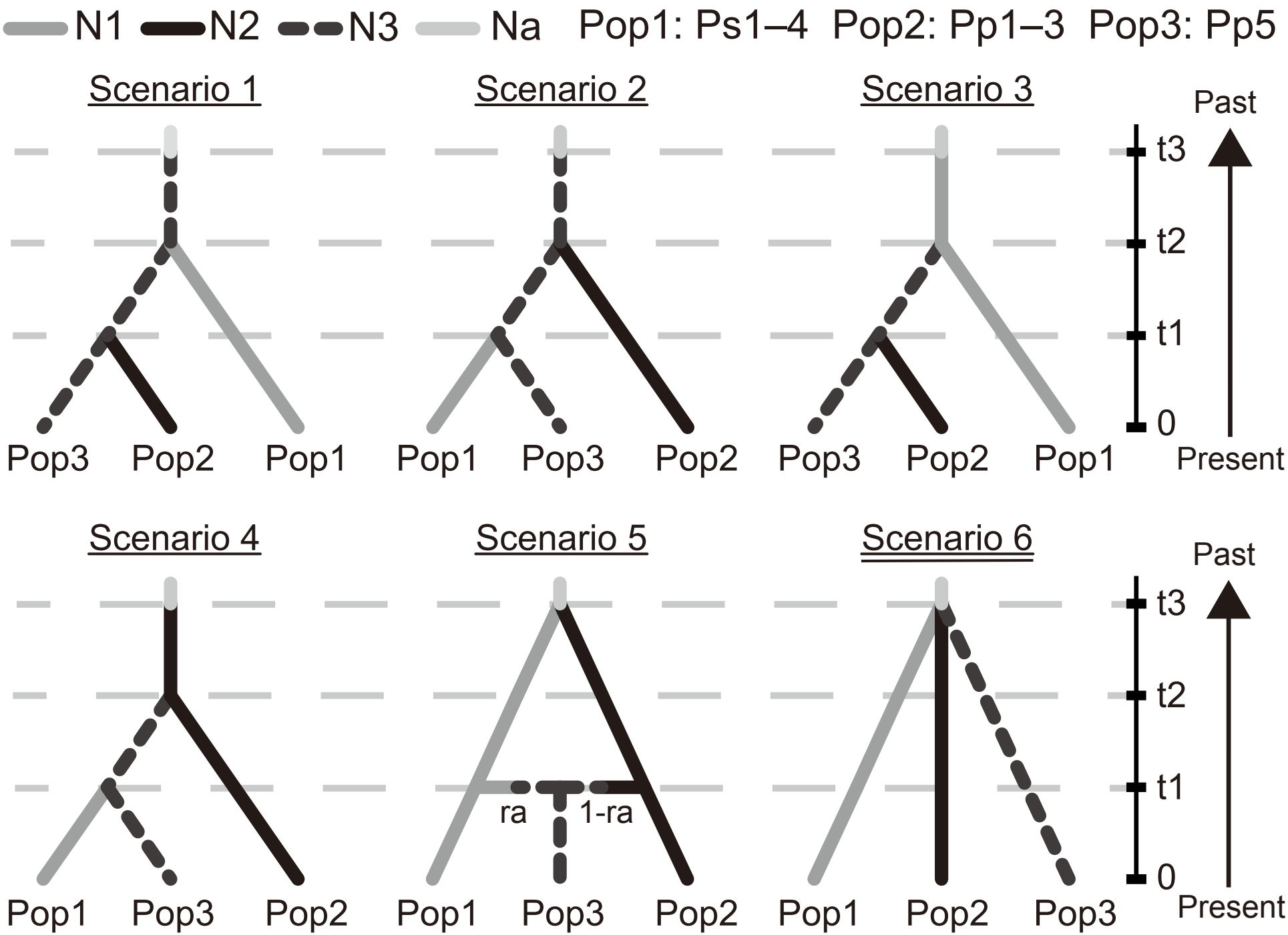
N1
N2
N3
Na
Pop1: Ps1–4
Pop2: Pp1–3
Pop3: Pp5
Scenario 1
Scenario 2
Scenario 3
Past
t3
t2
t1
0
Present
Pop3
Pop2
Pop1
Pop1
Pop3
Pop2
Pop3
Pop2
Pop1
Scenario 4
Scenario 5
Scenario 6
ra
1-ra
Pop1
Pop3
Pop2
Pop1
Pop3
Pop2
Pop1
Pop2
Pop3

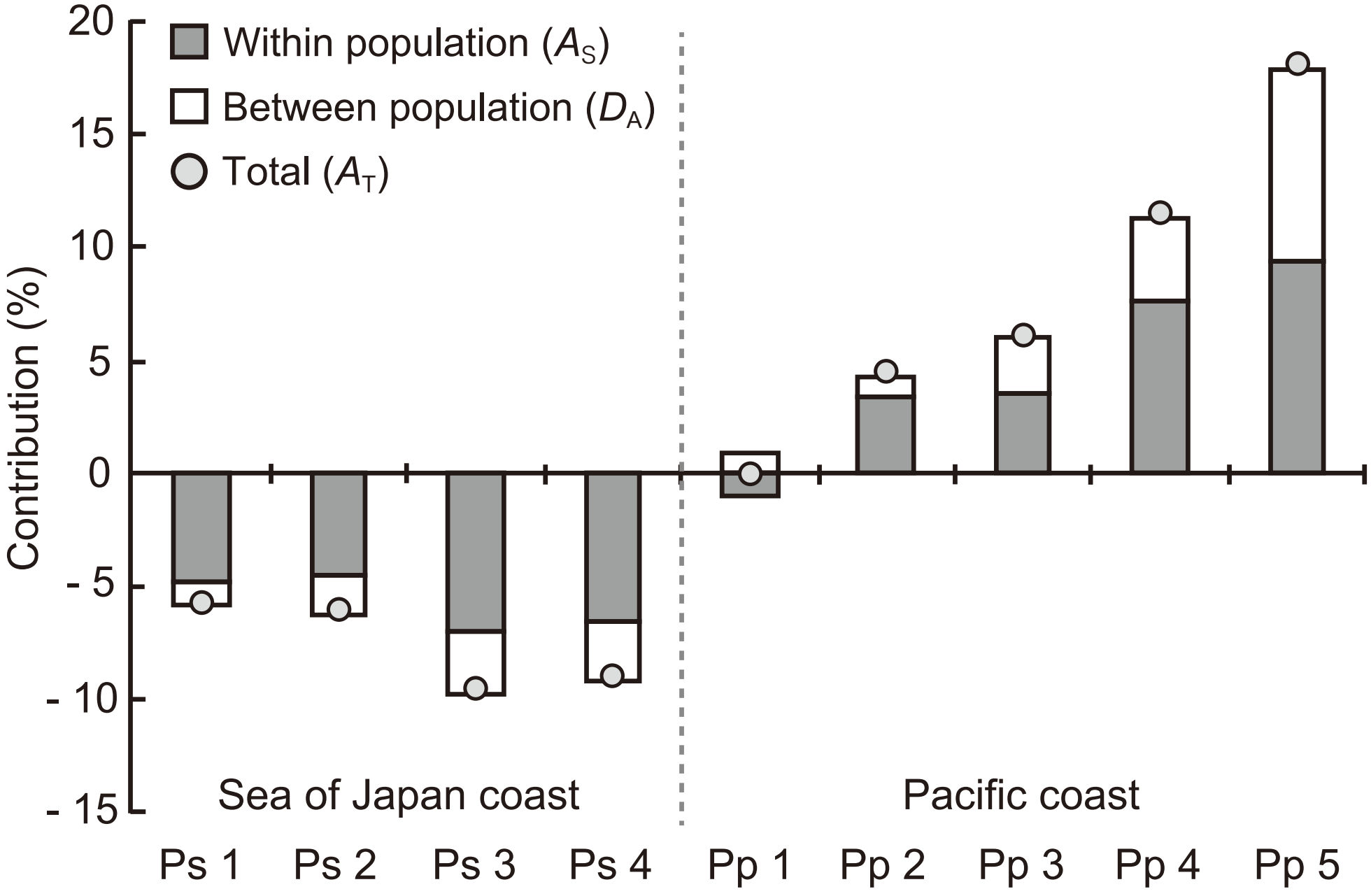
Within population (A_S)
Between population (D_A)
Total (A_T)
Contribution (%)
20
15
10
5
0
- 5
- 10
- 15
Sea of Japan coast
Pacific coast
Ps 1
Ps 2
Ps 3
Ps 4
Pp 1
Pp 2
Pp 3
Pp 4
Pp 5

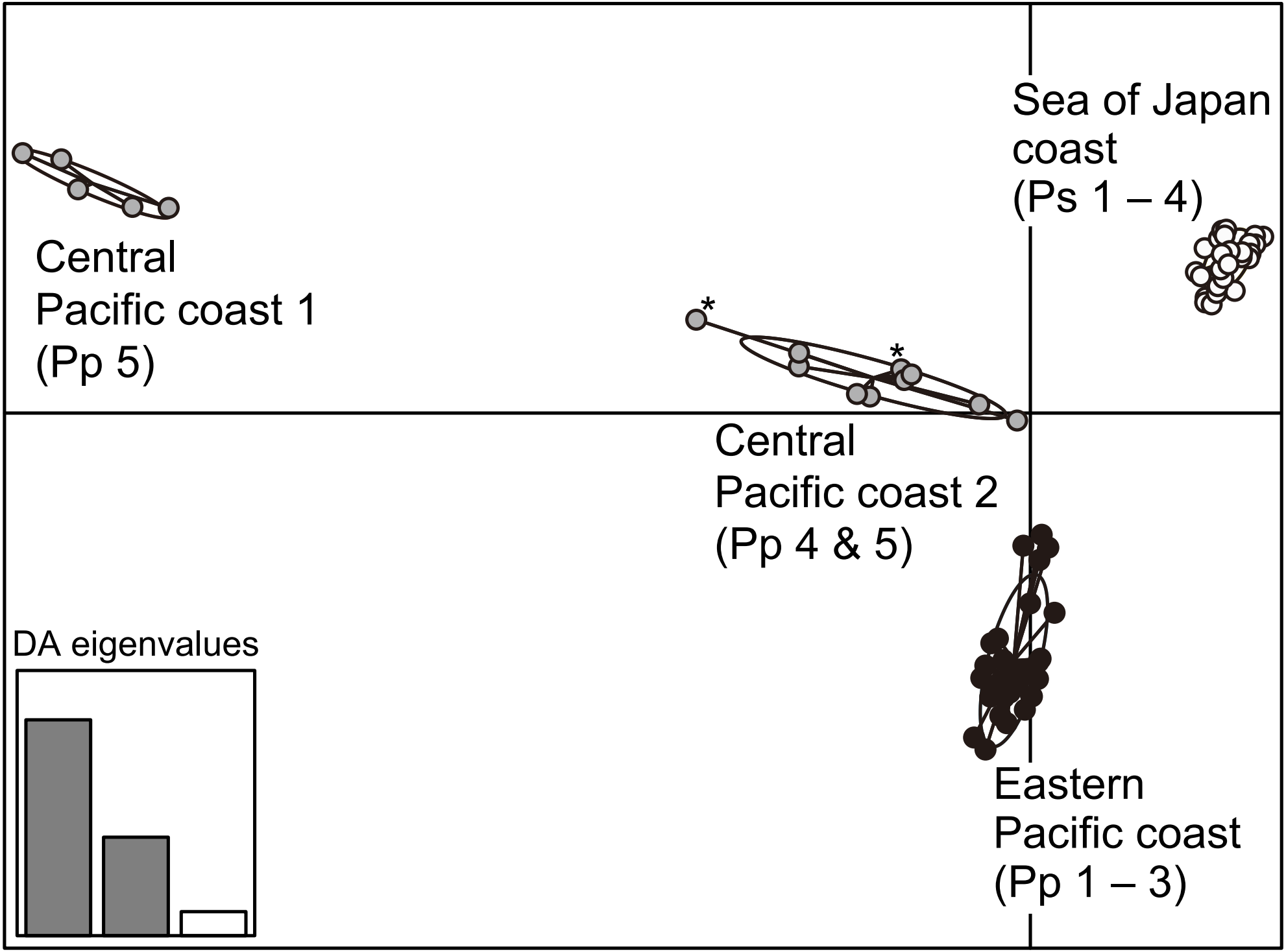
Sea of Japan
coast
(Ps 1 – 4)
Central
Pacific coast 1
(Pp 5)
Central
Pacific coast 2
(Pp 4 & 5)
Eastern
Pacific coast
(Pp 1 – 3)
DA eigenvalues

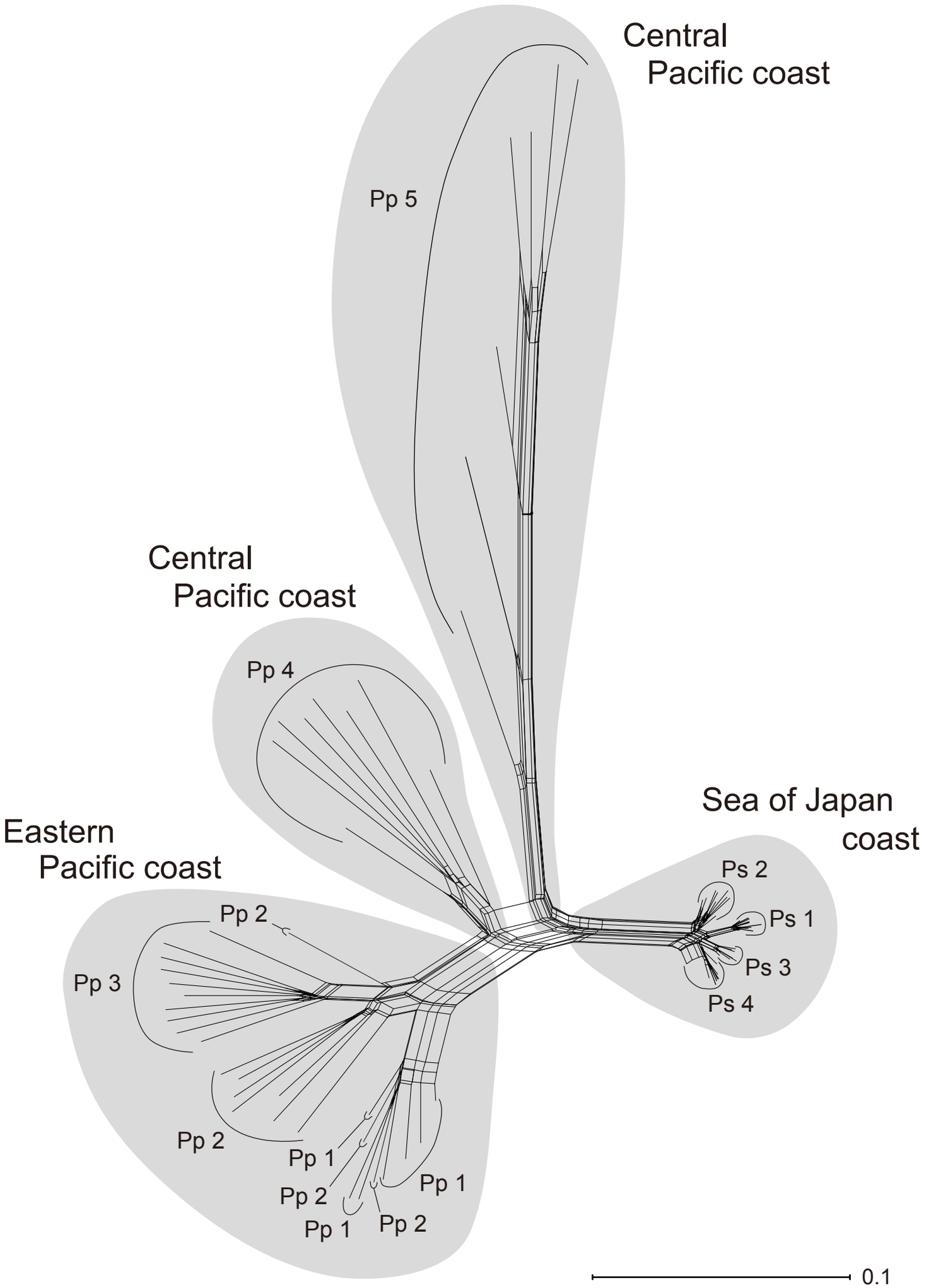
Central
Pacific coast
Pp 5
Central
Pacific coast
Pp 4
Sea of Japan
coast
Eastern
Pacific coast
Ps 2
Ps 1
Ps 3
Ps 4
Pp 2
Pp 3
Pp 2
Pp 1
Pp 2
Pp 1
Pp 1
Pp 2
0.1

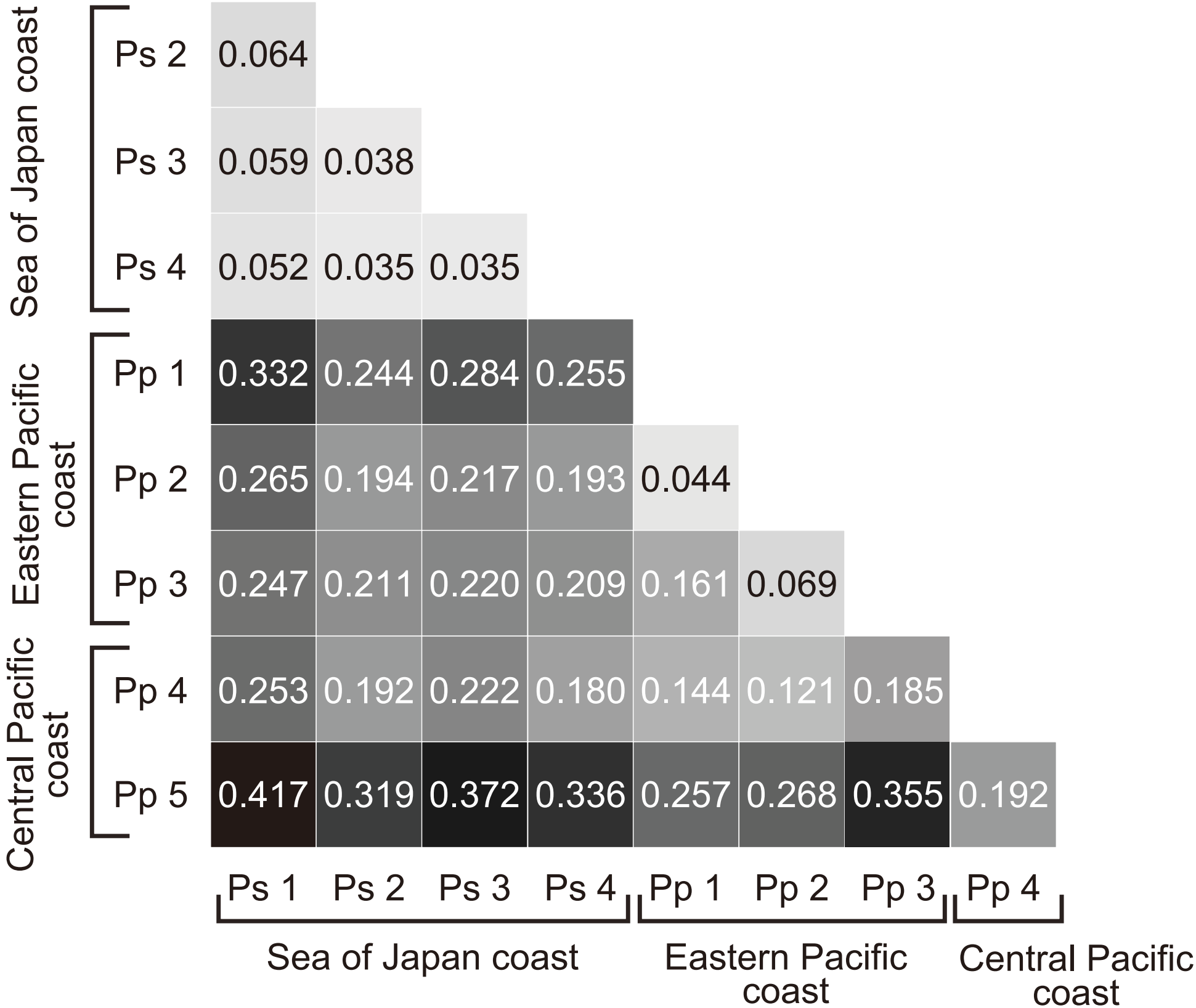
Sea of Japan coast
Eastern Pacific coast
Central Pacific coast
Ps 2
Ps 3
Ps 4
Pp 1
Pp 2
Pp 3
Pp 4
Pp 5
0.064
0.059 0.038
0.052 0.035 0.035
0.332 0.244 0.284 0.255
0.265 0.194 0.217 0.193 0.044
0.247 0.211 0.220 0.209 0.161 0.069
0.253 0.192 0.222 0.180 0.144 0.121 0.185
0.417 0.319 0.372 0.336 0.257 0.268 0.355 0.192
Ps 1 Ps 2 Ps 3 Ps 4 Pp 1 Pp 2 Pp 3 Pp 4
Sea of Japan coast
Eastern Pacific coast
Central Pacific coast

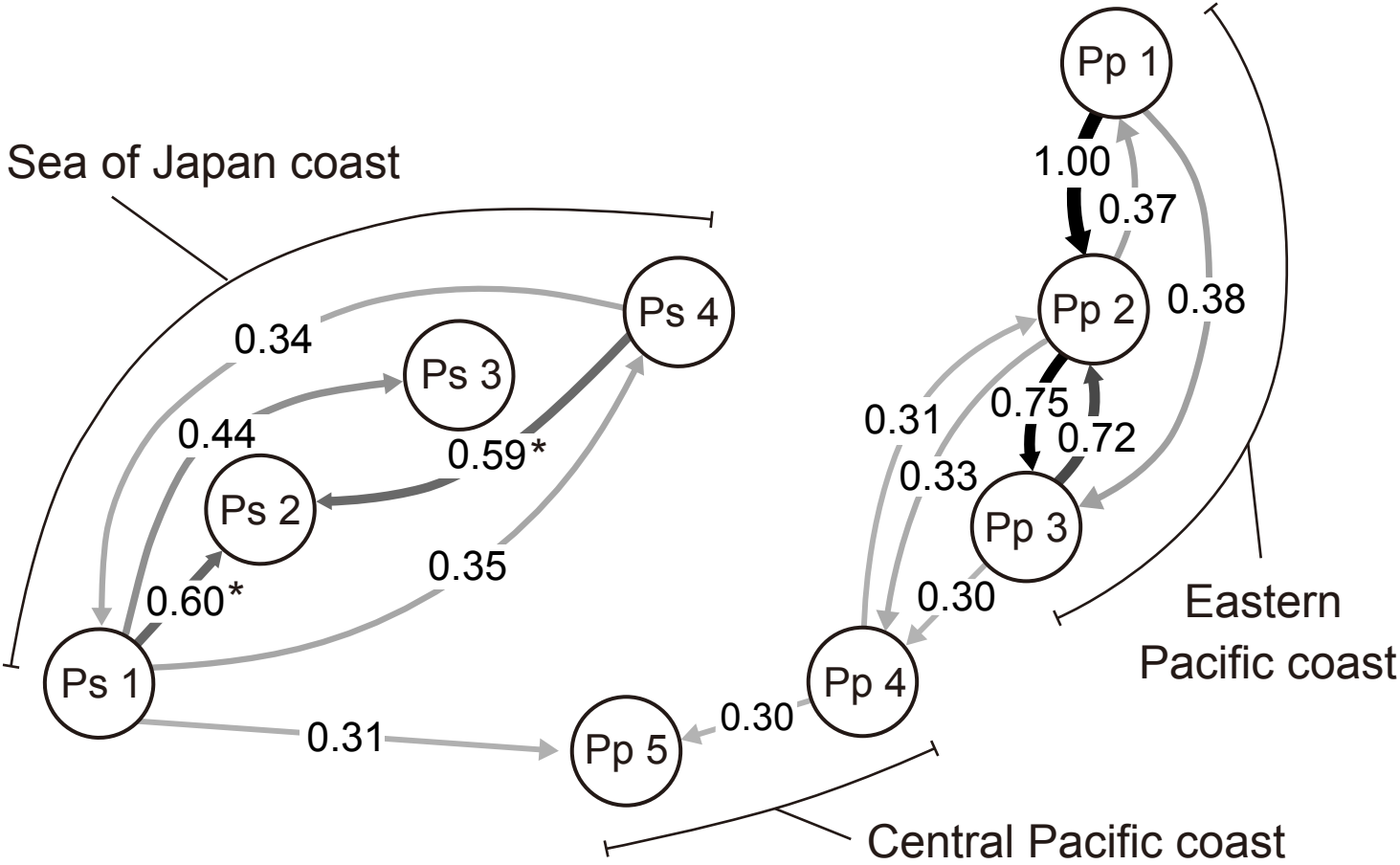
Sea of Japan coast
Ps 1
Ps 2
Ps 3
Ps 4
0.34
0.44
0.60*
0.59*
0.35
0.31
Pp 1
Pp 2
Pp 3
Pp 4
Pp 5
1.00
0.37
0.38
0.31
0.75
0.72
0.33
0.30
0.30
Eastern
Pacific coast
Central Pacific coast

Table S1. Samples information showing population code, locality, number of samples collected, and final dataset for analysis.

Population code	Locality	Coordinate	Date	No. of individuals	No. of individuals after the SNP calling	Population classification for DIYABC analysis	Accession no. of raw data of ddRad-seq
Ps 1	Itoshima, Fukuoka	33˚63’21 N 130˚18’17 E	November, 6–7, 2018 September, 13, 2019	10	9	POP 1	DRA012247
Ps 2	Shimonoseki, Yamagushi	34˚15’44 N 130˚89’76 E	June, 25, 2019	10	9	POP 1	DRA012248
Ps 3	Tomari, Tottori	35˚51’84 N 133˚94’87 E	June, 13, 2019	10	8	POP 1	DRA012249
Ps 4	Takano Kyoto,	35˚74’47 N 135˚11’10 E	June, 13, 2019	8	8	POP 1	DRA012250

Pp 1	Minami-sannrikucho, Miyagi	38˚38’42 N 141˚28’33 E	June, 19, 2019	10	7	POP 2	DRA012251
Pp 2	Iwaki, Fukushima,	36˚99’66 N 140˚98’11 E	May, 17, 2019	10	10	POP 2	DRA012252
Pp 3	Oharai, Ibaraki	36˚31’89 N 140˚59’30 E	May, 23, 2019	10	10	POP 2	DRA012253
Pp 4	Tateyama Chiba	34˚97’94 N 139˚82’20 E	June, 6, 2019	10	8	—	DRA012254
Pp 5	Shimoda, Shizuoka	34˚65’24 N 138˚96’47 E	June, 18, 2019	10	7	POP 3	DRA012255
Total				88	76		

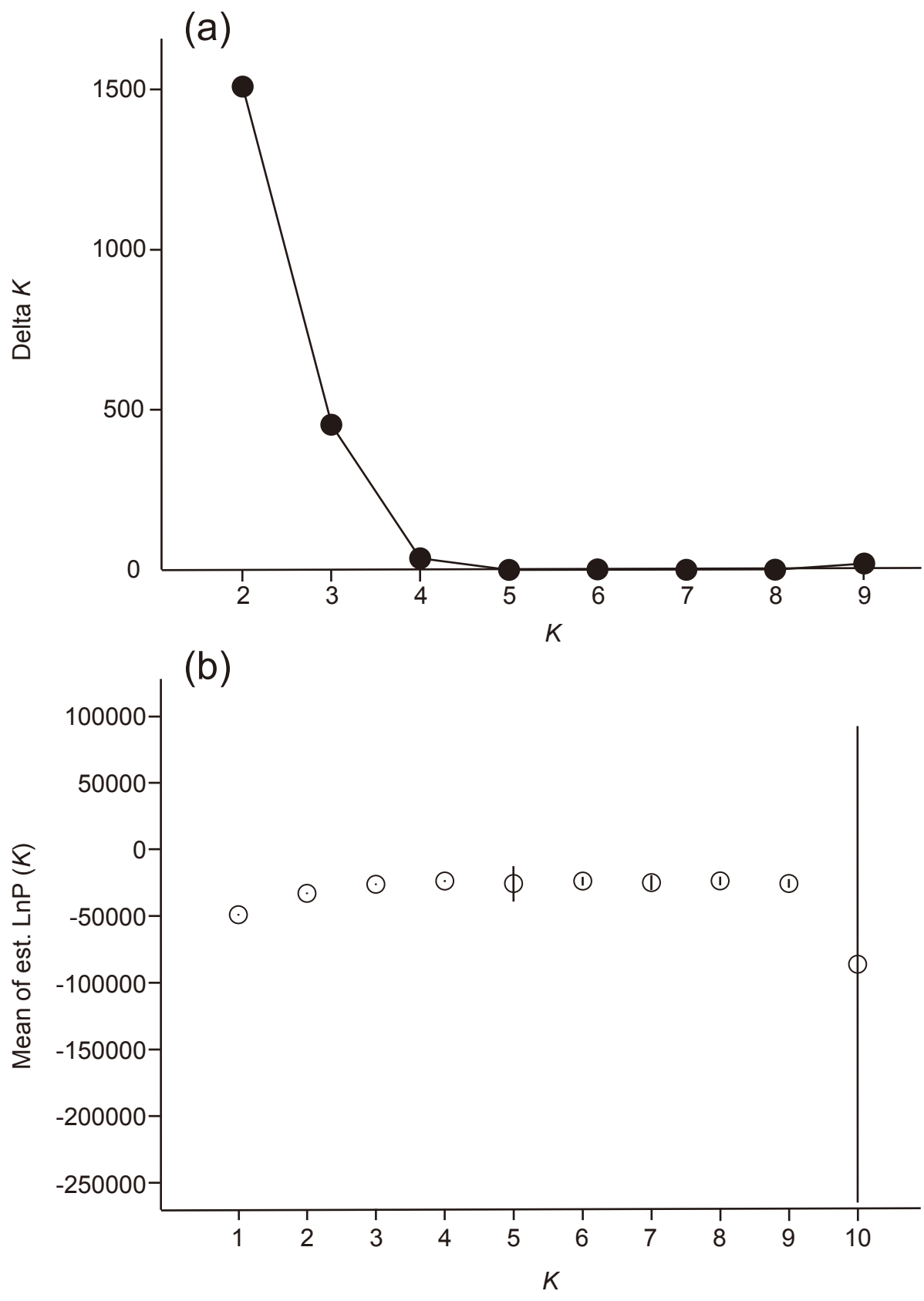

Fig. S1. Delta *K* values (a) and LnP (*K*) (b) in each of *K* cluster in STRUCTURE analysis.

Table S2. Prior distributions of the parameters used in DIYABC.

parameter	Probability distribution	Minimum	Maximum
Effective population size			
N1	uniform	10	50,000
N2	uniform	10	50,000
N3	uniform	10	50,000
Na	uniform	10	150,000
Time scale in generations			
t1	uniform	10	50,000
t2	uniform	10	100,000
t3	uniform	10	100,000
Admixture			
ra	uniform	0.1	0.9

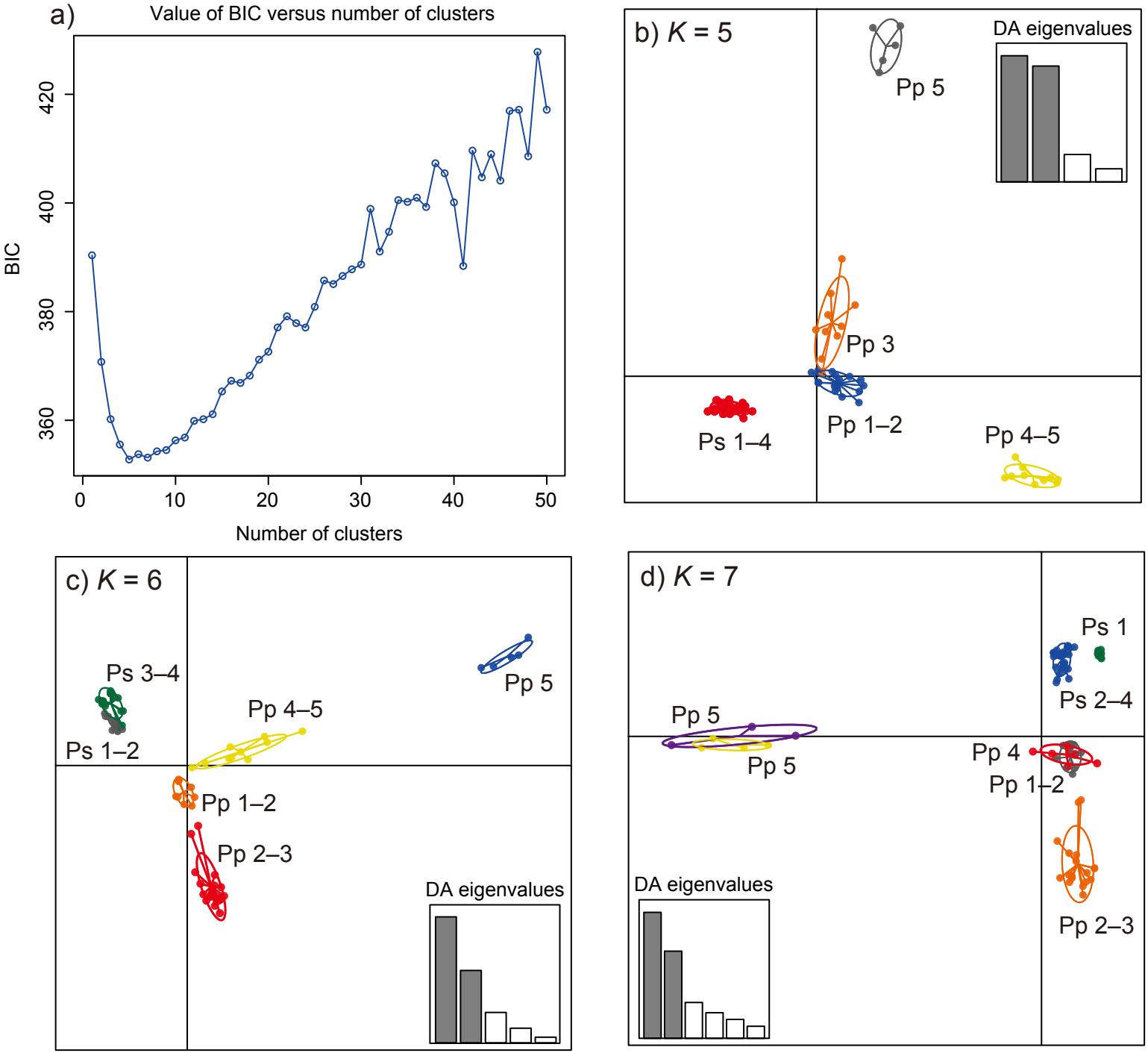

Fig. S2. BIC values in each of *K* cluster (a). Discriminant analysis of principal components scatter plot at *K* = 5 (b), *K* = 6 (c), and *K* = 7 (d) based on the *Eisenia bicyclis* collected in the present study.

Table S3. Original demographic parameters estimated by DIYABC in Scenario 6.

Parameter		Mean	Median	Mode	Quantile 2.5%	Quantile 5.0%	Quantile 95.0%	Quantile 97.5%
Effective population size	N1	9,690	9,770	9,730	4,570	5,620	13,500	14,100
	N2	34,800	35,300	36,300	22,800	25,300	42,700	45,100
	N3	37,700	39,000	45,900	18,400	22,000	49,000	49,500
	Na	144,000	145,000	146,000	129,000	134,000	149,000	150,000
Time scale in generations	t1	12,200	9,400	373	375	708	33,500	38,300
	t2	28,400	28,800	34,900	5,580	8,180	47,800	51,100
	t3	43,400	44,000	45,900	24,600	28,100	56,800	60,000

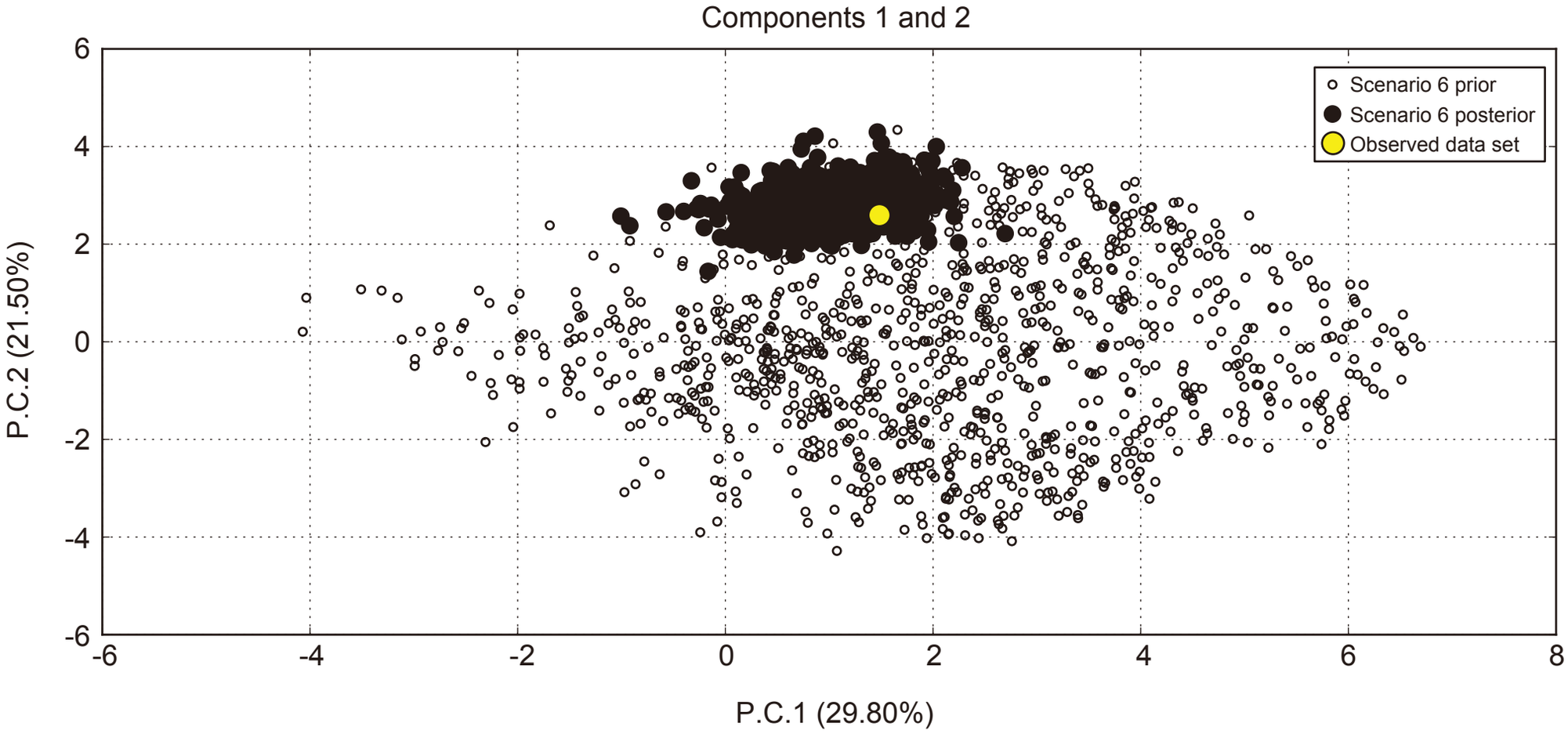

Fig. S3. PCA on summary statistics of the best-supported scenario 6 based on 1,000 simulations in DIYABC analysis.